Nonlinear Dyn
https://doi.org/10.1007/s11071-024-10115-x

RESEARCH

Periodic solutions of photo-gravitational R4BP with variable mass and Stokes drag

Bao Ma · Elbaz I. Abouelmagd · Fabao Gao

Received: 15 March 2024 / Accepted: 30 July 2024

Abstract The present paper describes the motion of an infinitesimal body in the framework of restricted four-body problem, incorporating perturbations from photo-gravitational, variable mass, and Stokes drag effects. Dynamic equations governing a fourth body with changing mass are obtained using Jeans' law and Meshcherskii space-time transformations. The locations of the Lagrangian points and their evolution under variations of the aforementioned perturbations have been numerically studied, revealing the sensitivity of the locations and quantities of Lagrangian points to these varying parameters. Furthermore, the stability of Lagrangian points in the linear sense has been investigated, and it has been found that all Lagrangian points considered in this study are unstable. The zero-velocity curves have also been studied as a function of the Jacobian integral constant. As this constant decreases, the Hill region becomes larger. The Lindstedt–Poincaré method is applied to calculate the perturbation solutions near non-collinear Lagrangian points, yielding second- and third-order periodic solutions. A numerical work is conducted to track the evolution of periodic solutions near non-collinear Lagrangian points with variable mass parameter γ. It demonstrates that a substantial increase in γ results in a larger area surrounding the periodic solutions of the triangular Lagrangian points, exhibiting a visually regular elliptical shape. Conversely, a decrease in γ leads to a reduction in the region of periodic solutions, accompanied by notable alterations in shape, particularly concerning third-order periodic solutions.

Keywords R4BP · Lagrangian point · Periodic solution · Stokes drag · Photo-gravitational

B. Ma · F. Gao (✉)
School of Mathematical Science, Yangzhou University, Yangzhou 225002, China
e-mail: gaofabao@sina.com

B. Ma
e-mail: mabaoyzu@163.com

E. I. Abouelmagd
Celestial Mechanics and Space Dynamics Research Group (CMSDRG), Astronomy Department, National Research Institute of Astronomy and Geophysics (NRIAG), Helwan 11421, Cairo, Egypt
e-mail: eabouelmagd@gmail.com; elbaz.abouelmagd@nriag.sci.eg

1 Introduction

The three-body problem is a complex dynamic problem, which refers to the motion of three particles interacting in a particle system first proposed by the French astronomer Laplace in the 18th century when studying the planetary motion in the solar system. Later, French mathematician Poincaré conducted extensive research on this issue. Due to the inability to obtain analytical solutions for the general three-body problems, a new branch of the R3BP (abbreviated form of restricted three-body problem) is obtained by simplifying the problem. The R4BP refers to the motion of an infinitesimal mass under the gravitational force of three large celestial bodies, often called the primaries, and the tiny body does not affect the primaries' motion. Furthermore, if the mass of an infinitesimal body changes over time, the problem becomes a variable-mass R4BP.

The study of Lagrangian points is of great significance in the study and application of celestial mechanics, including in variable-mass R4BP. The Lagrangian point refers to the points in a celestial system where an object can remain stationary relative to the system reference frame. Italian mathematician Joseph Lagrange first studied it, which has great significance and applications. For example, in a three-body system such as the Sun, Earth, and Moon, five Lagrangian points can be used to place space stations, artificial satellites, astronomical telescopes, and so on [1,2], which are very useful for aerospace dynamics and deep space exploration. In recent years, scientists have conducted many studies on Lagrangian points and made many of the latest advances [3].

The numerical methods are used to study how the oblate primary and prolate primary parameters affect Lagrangian points' positions and linear stability [4,5]. The Lagrangian point dynamics of the R3BP with equally massed prolate radiating bodies were studied in [6]. The linear stability and positions of the co-planar Lagrangian points were determined using numerical methods. The results showed that these two parameters have a great influence on the system's Lagrangian point dynamics. In [7], the authors mainly studied the linear stability of Lagrangian points in the generalized photo-gravitational Chermnykh-like issue with the power-law. The positions and velocity sensitivities under the effect of radiation and oblate primaries in the R3BP are also studied in [8]. Recently in [9], the authors considered the elliptical R3BP under radiation pressure and the primaries oblateness perturbation, obtained the location of non-collinear Lagrangian points and approximate analytical solutions nearby, and applied them to real astronomical systems. It was found that the stability and locations of the Lagrangian points will be significantly affected by changes in disturbance parameters. While within the framework of quantized Hill's three-body problem, the stability of equilibrium points and their in-plane and out-of-plane motion was also studied [10].

In the framework of R4BP, the position and existence of the Lagrangian points are studied under the effect of non-spherical shapes of the primaries in [11,12]. The stability of these points is also investigated with photo-gravitational and Stokes drag perturbations, where three primary bodies have radiation, and the Stokes force is a dissipative force in [13]. Many studies have addressed on this problem under the effect of various perturbations. For example, but not limited to, the existence and position of Lagrangian points in variable mass, as well as the zero-velocity curve, were studied in [14], where the position lines of the three primary bodies form an equilateral triangle and the second and third bodies have the same mass. It was found that there are eight Lagrangian points, and the parameter of variable mass affects the position of the points. While considerable studies are preformed in [15,16] under the effect of photo-gravitational and Stokes forces to analysis these effects on the positions change of Lagrangian points and the variation of the zero-velocity curves.

The periodic solution of R3BP provides a theoretically rich and complex system, and the study of periodic solutions can be useful for planning space missions. Some artificial satellites and space probes are placed on Lagrangian points or other stable periodic solutions better to observe targets such as the Sun and Earth or to provide a more stable environment for scientific experiments. These points and related periodic solutions are evaluated as the optimal positions to transfer the spacecraft to the nominal periodic solution or related stable manifold. In this context, the heteroclinic connections between quasi-periodic solutions are calculated [17]. Also outstanding study are carried out to analysis the positions of collinear Lagrangian points and their periodic solutions under the effect of triaxial rigid body parameters in the R3BP, and numerical simulation results were provided [18]. But the periodic solutions in the framework of quantized R3BPs are investigated [19]. The LP and differential corrector methods are used to find a family of halo solutions at artificial Sun–Earth L_2 points [20]. Furthermore, periodic solutions and bifurcation analysis of R3BPs under triaxial and radial perturbations are calculated in [21]. Also, the LP method is used to calculate the approximate analytical periodic solutions of R3BP under oblateness, radiation pressure, and variable mass perturbations [22].

The analysis of periodic solutions is not exclusive to R3BP but also a great appearance in four-body problem. In [23], the authors used numerical methods to study the existence of periodic solutions for R4BPs with equilateral triangle configurations. While in [24], the authors used the Fourier series method to determine the periodic solutions around collinear

Lagrangian points in the spatial collinear R4BP with non-spherical primaries. Recently in [25], the authors studied perturbed two-body solutions and R3BPs orbits and proved that if the perturbation force is conserved or the corresponding motion has its extended Jacobian integral, the first and second types of orbits in the rotating Kepler problem will always exist. In [26], the authors studied the perturbed relative motion, obtained the interior loops of the periodic solutions using the numerical method, and analyzed its stability. In addition, the Poincaré surface of sections is used to study the stability of periodic solutions under the parameters of the eccentricity of the primaries' trajectory, solar radiation pressure, and the Jacobian constant perturbations [27]. Some interesting research that enriches readers' knowledge of space dynamics and celestial mechanics are addressed in [28–38].

When studying Lagrangian points in R4BPs, existing literature has predominantly focused on individual perturbation factors such as photo-gravitational effects, variable mass, and Stokes drag, with limited attention given to their combined influence. While scholars have extensively examined periodic solutions in proximity to collinear Lagrange points, there remains a notable gap in the exploration of periodic solutions near non-collinear Lagrangian points. In light of this, our study aims to analyze Lagrangian points and periodic solutions near non-collinear points, considering the combined perturbations of photo-gravitational forces, variable mass effects, and Stokes drag. We anticipate that this study will contribute helpful insights to this domain.

In this paper, Sect. 1 is introduction. Section 2 presents the motion equations of the variable-mass R4BP under photo-gravitational and Stokes force perturbations. Section 3 calculates the Lagrangian points and their evolution under the variation of variable mass, photogravitational, and Stokes force parameters. Section 4 is about the linear stability of Lagrangian points. Section 5 is the zero-velocity curve, and the Sect. 6 calculates periodic solutions near non-collinear Lagrangian points. The last Sect. 7 is the conclusion.

2 Equations of motion

We will now explore the motion of variable mass within the framework of a R4BP in a Lagrangian configuration. Here, the three primaries involved are radiating and located at the vertices of an equilateral triangle. Let m_i $(i = 1, 2, 3)$ represent the masses of the three primaries, assuming that $m_1 \geq m_2 = m_3$, and they are moving along circular orbits around their common center of masses. We denote the mass of a fourth body by m, which is negligible compared to the primaries' masses. In this context, the fourth body is moving under the gravitational attraction forces of the three primaries without affecting their motion.

Furthermore, we have chosen the combined mass of the primaries and the distance between them as our units for mass and length and the time unit is selected to set the gravitational constant to unity. Assuming $m_2/(m_1 + m_2 + m_3) = m_3/(m_1 + m_2 + m_3) = \mu$, $m_1 + m_2 + m_3 = 1$, then $m_1 = 1 - 2\mu$. In synodic coordinates, we impose that also the coordinates of the infinitesimal body (fourth body) are represented by (X, Y), while those of the primaries, denoted as (X_i, Y_i), where

$$\begin{aligned}
&(X_1, Y_1) = (\sqrt{3}\,\mu, 0),\\
&(X_2, Y_2) = \left(-\frac{\sqrt{3}}{2}(1-2\,\mu), -\frac{1}{2}\right),\\
&(X_3, Y_3) = \left(-\frac{\sqrt{3}}{2}(1-2\,\mu), \frac{1}{2}\right).
\end{aligned} \tag{1}$$

Thus, the equations of motion of the infinitesimal mass m under the effects of photo-gravitational and Stokes drag in a rotating coordinate can be described in the dimensionless variables as [13,16]

$$\begin{aligned}
&\ddot{X} - 2\dot{Y} + \frac{\dot{m}}{m}(\dot{X} - Y) = W_X + S_X,\\
&\ddot{Y} + 2\dot{X} + \frac{\dot{m}}{m}(\dot{Y} + X) = W_Y + S_Y,
\end{aligned} \tag{2}$$

where the function W is defined by

$$\begin{aligned}
W(X, Y) = &\frac{1}{2}(X^2 + Y^2) + \frac{(1-2\mu)q_1}{d_1}\\
&+\frac{\mu q_2}{d_2} + \frac{\mu q_3}{d_3},
\end{aligned} \tag{3}$$

here $q_i \in (0, 1]$ $(i = 1, 2, 3)$ being constant implies the neglect of fluctuations in radiation beams, the shadow effect of primaries, and the assumption of purely radial radiation. The radiation pressure, denoted as F_{p_i}, acting on a primary can be expressed in terms of the gravitational attraction force, F_{g_i}, as $F_{p_i} = F_{g_i}(1 - q_i)$. Here, F_{p_i} represents the radiation pressure due to the primary, and F_{g_i} signifies the gravitational force acting on the primary. The parameter $q_i = 1 - p_i = 1 - F_{p_i}/F_{g_i}$, a constant specific to the given primary, serves as a reduction factor determined by the primary's radius a, density δ, and radiation-pressure efficiency factor x in the cgs system, where $q_i = 1 - 5.6 \times 10^{-3} x/(a\delta)$ (See [39] and the references therein for more details).

By using Eq. (1), the separation distances among the infinitesimal mass and primaries d_1, d_2, and d_3 are defined by

$$
\begin{aligned}
d_1^2 &= \left(X - \sqrt{3}\mu\right)^2 + Y^2, \\
d_2^2 &= \left[X + \frac{\sqrt{3}}{2}(1-2\mu)\right]^2 + \left(Y + \frac{1}{2}\right)^2, \\
d_3^2 &= \left[X + \frac{\sqrt{3}}{2}(1-2\mu)\right]^2 + \left(Y - \frac{1}{2}\right)^2.
\end{aligned} \tag{4}
$$

The perturbed acceleration components of the Stokes drag force in the X and Y directions are given by Murray [40]

$$
\begin{aligned}
S_X &= -k\left(\dot{X} - Y + \sigma H_Y\right) \\
&= -k\left(\dot{X} - Y - \frac{3\sigma Y}{2d^{7/2}}\right), \\
S_Y &= -k\left(X + \dot{Y} - \sigma H_X\right) \\
&= -k\left(\dot{Y} + X + \frac{3\sigma X}{2d^{7/2}}\right),
\end{aligned} \tag{5}
$$

where H and d are two functions in variables X and Y and are defined by

$$
\begin{aligned}
H(X, Y) &= \left(X^2 + Y^2\right)^{-3/4}, \\
d(X, Y) &= \sqrt{X^2 + Y^2},
\end{aligned} \tag{6}
$$

k is the dissipative constant with rang values Beaugé (1993) ($0 < k < 1$) [41], σ is the ratio of the gas and Kepler velocities Murray [40].

The Jeans' law and Meshcherskii space-time transformations preserve the dimension of space and time. Now, we impose that the mass of the infinitesimal body varies with time t according to Jean's law: $dm/dt = -\alpha\, m^n$, where α is constant and the value $n \in [0.4, 4.4]$ (for the star of the main sequence). For a rocket, $n = 1$, and the mass of the rocket varies exponentially as $m = m_0 e^{-\alpha t}$, m_0 is the initial mass. The classic law mainly taken from James Jeans' monumental work [42]. Despite its empirical basis, a meticulous examination of the monograph reveals a minimal deviation between theoretical calculations and observed data. This precision underscores its status as a classic law that continues to be widely utilized. In recent years, researchers have utilized nonparametric statistical testing methods, rather than empirical approaches, to analyze and interpret natural satellite data, resulting in the derivation of alternative variable mass laws with high credibility. For further details, please refer to [43–47].

Now, the Meshcherskii space-time transformations are used to simplify the equations: $u = X\gamma^q$, $v = Y\gamma^q$, $d\tau = \gamma^{\bar{k}} dt$, $d_i = \gamma^{-q} R_i$, $i = 1, 2, 3$, where γ represents the ratio of the primary's mass at time t to its initial mass [48].

Let $n = 1$, $\bar{k} = 0$, $q = 1/2$ in keeping with the work by Singh and Ishwar [49], the velocity and acceleration components can be written as

$$
\begin{aligned}
\gamma^{1/2}\dot{X} &= u' + \frac{1}{2}\alpha\, u, \\
\gamma^{1/2}\dot{Y} &= v' + \frac{1}{2}\alpha\, v, \\
\gamma^{1/2}\ddot{X} &= u'' + \alpha u' + \frac{1}{4}\alpha^2\, u, \\
\gamma^{1/2}\ddot{Y} &= v'' + \alpha v' + \frac{1}{4}\alpha^2\, v,
\end{aligned} \tag{7}
$$

where the dot (.) and prime ($'$) represent the derivative with respect to t and τ, respectively, after utilizing Eqs. (2–7), then equations of motion can be rewritten in the following form

$$
\begin{aligned}
\ddot{u} - 2\dot{v} &= \Omega_u + S_u, \\
\ddot{v} + 2\dot{u} &= \Omega_v + S_v,
\end{aligned} \tag{8}
$$

where

$$
\begin{aligned}
\Omega(u, v) = &\frac{1}{2}\left(1 + \frac{\alpha^2}{4}\right)\left(u^2 + v^2\right) \\
&+ \gamma^{3/2}\left[\frac{(1-2\mu)q_1}{R_1} + \frac{\mu q_2}{R_2} + \frac{\mu q_3}{R_3}\right],
\end{aligned} \tag{9}
$$

$$
\begin{aligned}
S_u &= -k\left[\dot{u} + \frac{\alpha u}{2} - v\left(1 + \frac{3\sigma\gamma^{7/4}}{2R_0^{7/2}}\right)\right], \\
S_v &= -k\left[\dot{v} + \frac{\alpha v}{2} + u\left(1 + \frac{3\sigma\gamma^{7/4}}{2R_0^{7/2}}\right)\right],
\end{aligned} \tag{10}
$$

and

$$
\begin{aligned}
R_0 &= \sqrt{u^2+v^2},\\
R_1^2 &= \left(u-\sqrt{3}\mu\sqrt{\gamma}\right)^2+v^2,\\
R_2^2 &= \left[u+\frac{\sqrt{3}}{2}(1-2\mu)\sqrt{\gamma}\right]^2+\left(v+\frac{\sqrt{\gamma}}{2}\right)^2,\\
R_3^2 &= \left[u+\frac{\sqrt{3}}{2}(1-2\mu)\sqrt{\gamma}\right]^2+\left(v-\frac{\sqrt{\gamma}}{2}\right)^2.
\end{aligned}
\tag{11}
$$

System (8) represents a generalized dynamical system for the motion of variable mass in the framework of R4BP under the perturbation effects of Stokes drag and photo-gravitational forces. Its mass variation is also a source for motion's perturbation. This system reduced to many sub-models or special cases as follows:

- When $q_1=q_2=q_3=1$, the equations are convenient with the obtained system in [16].
- When $k=0$, the equations are convenient with the obtained system in [15].
- When $\alpha=0,\ \gamma=1$, the equations are convenient with the obtained system in [13].
- When $k=0,\ q_1=q_2=q_3=1$, the equations are convenient with the obtained system in [14].

By multiplying the first and second equations of (8) by $2\dot{u}$ and $2\dot{v}$, respectively, and adding them together, after integration, we obtain a quasi-integral for motion which is similar to Jacobian integral.

$$
\dot{u}^2+\dot{v}^2=2(S+\Omega)-C-2\int_0^t\frac{\partial}{\partial t}(S+\Omega)dt, \tag{12}
$$

where C denotes the Jacobian integral constant when the last term in Eq. (12) is either equals zero or can be calculated.

3 Lagrangian points

Investigating the Lagrangian points and their stability is very meaningful because many qualitative analyses of dynamic systems are carried around them, including the computation of periodic solutions in their vicinity. A Lagrangian point refers to a location where both velocity and acceleration are zero, i.e. $\dot{x}=\dot{y}=\ddot{x}=\ddot{y}$. Lagrangian points lie on the u-axis are called the collinear Lagrangian points, otherwise called the non-collinear ones. In this section, we will investigate the Lagrangian points of the infinitesimal mass body with photo-gravitational, Stokes drag, and variable mass perturbations

Substituting Eqs. (9–11) into righthand sides of Eq. (8), we get

$$
\begin{aligned}
\Omega_u+S_u &= T_{u1}+T_{u2}+T_{u3}+T_{u4}+T_{u5},\\
\Omega_v+S_v &= T_{v1}+T_{v2}+T_{v3}+T_{v4}+T_{v5},
\end{aligned}
\tag{13}
$$

where

$$
\begin{aligned}
T_{u1} &= \left(\frac{\alpha^2}{4}+1\right)u,\\
T_{u2} &= \frac{\gamma^{3/2}q_1(2\mu-1)\left(u-\sqrt{3\gamma}\mu\right)}{\left[\left(u-\sqrt{3\gamma}\mu\right)^2+v^2\right]^{3/2}},\\
T_{u3} &= \frac{\gamma^{3/2}q_2\,\mu\left[\frac{\sqrt{3\gamma}}{2}(2\mu-1)-u\right]}{\left[\left(\frac{\sqrt{3\gamma}}{2}(1-2\mu)+u\right)^2+\left(v+\frac{\sqrt{\gamma}}{2}\right)^2\right]^{3/2}},\\
T_{u4} &= \frac{\gamma^{3/2}q_3\,\mu\left[\frac{\sqrt{3\gamma}}{2}(2\mu-1)-u\right]}{\left[\left(\frac{\sqrt{3\gamma}}{2}(1-2\mu)+u\right)^2+\left(v-\frac{\sqrt{\gamma}}{2}\right)^2\right]^{3/2}},\\
T_{u5} &= k\left[\frac{\alpha\,u}{2}-v\left(1+\frac{3\gamma^{7/4}\sigma}{2\left(u^2+v^2\right)^{7/4}}\right)\right],
\end{aligned}
\tag{14}
$$

and

$$
\begin{aligned}
T_{v1} &= \left(\frac{\alpha^2}{4}+1\right)v,\\
T_{v2} &= \frac{\gamma^{3/2}q_1(2\mu-1)v}{\left[\left(u-\sqrt{3\gamma}\mu\right)^2+v^2\right]^{3/2}},\\
T_{v3} &= \frac{-\gamma^{3/2}q_2\,\mu\left(v+\frac{\sqrt{\gamma}}{2}\right)}{\left[\left(\frac{\sqrt{3\gamma}}{2}(1-2\mu)+u\right)^2+\left(v+\frac{\sqrt{\gamma}}{2}\right)^2\right]^{3/2}},\\
T_{v4} &= \frac{-\gamma^{3/2}q_3\,\mu\left(v-\frac{\sqrt{\gamma}}{2}\right)}{\left[\left(\frac{\sqrt{3\gamma}}{2}(1-2\mu)+u\right)^2+\left(v-\frac{\sqrt{\gamma}}{2}\right)^2\right]^{3/2}},\\
T_{v5} &= -k\left[\frac{\alpha\,v}{2}+u\left(1+\frac{3\gamma^{7/4}\sigma}{2\left(u^2+v^2\right)^{7/4}}\right)\right].
\end{aligned}
\tag{15}
$$

Now, substitute Eqs. (14, 15) into Eq. (13) and let $\Omega_u+S_u=0$ and $\Omega_v+S_v=0$. Then, the obtained roots are the Lagrangian points.

Fig. 1 The positions of Lagrangian points with $\gamma = 0.15, \alpha = 2.2, \sigma = 0.018, k = 0.000005, q_1 = 0.98, q_2 = 0.975, q_3 = 0.975$, and different mass ratio parameters μ

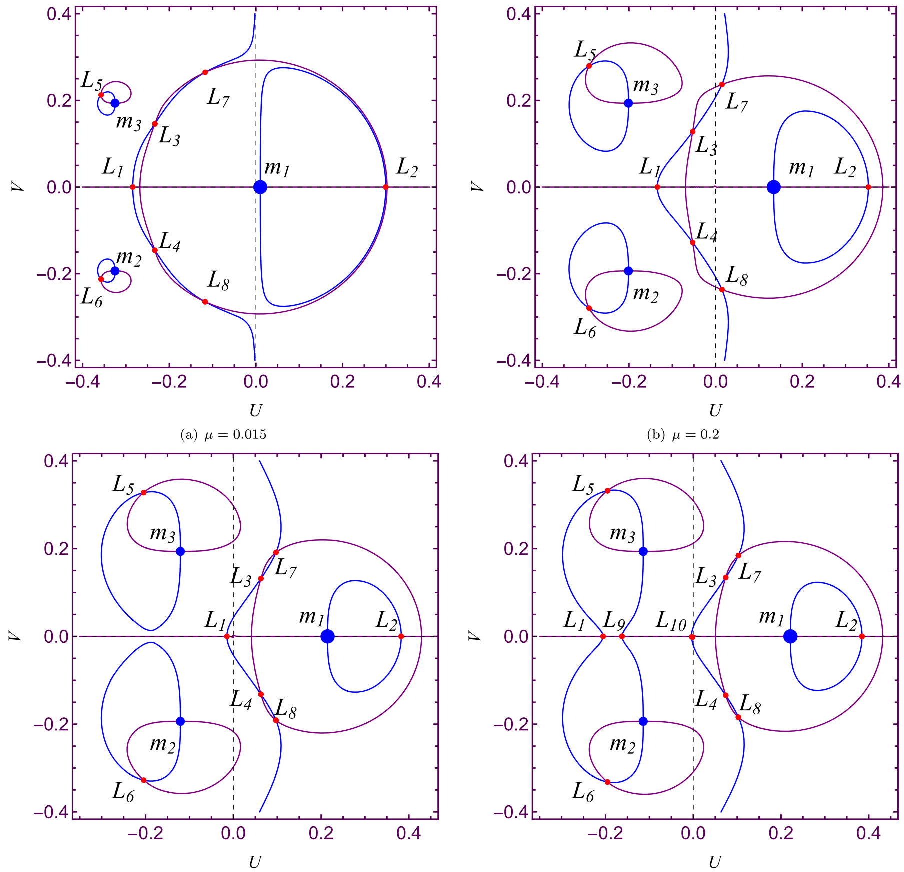

(a) $\mu = 0.015$

(b) $\mu = 0.2$

(c) $\mu = 0.32$

(d) $\mu = 0.33$

The parameters's values are within the range $0 < \mu \leq 1/3, 0 < \gamma < 1, 0 < \alpha \leq 2.2, 0 < \sigma < 1, 0 < q_1, q_2, q_3 \leq 1$. Constraining α within this specified range aims to effectively capture the intricate dynamic characteristics and evolutionary processes within the celestial system, thereby ensuring the rationality and accuracy of the model employed. For further details, please refer to [14,50,51] and the references therein.

We employed a numerical method to determine the positions of Lagrangian points within the proposed system. Typically, there exist eight or ten Lagrangian points, all of which are non-collinear. The number of Lagrangian points obtained varies with different parameter values, as illustrated in Figs. 1, 2, 3, 4 and 5. In these figures, the blue dots represent the primaries, while the red dots indicate the Lagrangian points.

In Fig. 1, set $\gamma = 0.15, \alpha = 2.2, \sigma = 0.018, k = 0.000005, q_1 = 0.98, q_2 = 0.975, q_3 = 0.975$. When $\mu = 0.015$, there are eight non-collinear Lagrangian points in Fig. 1a and no collinear Lagrangian points. When μ increased to 0.2 and 0.32, there were still only eight non-collinear Lagrangian points, as shown in Fig. 1b, c. However, when $\mu = 0.33$, ten non-collinear Lagrangian points appeared, adding two more non-collinear Lagrangian points, L_1 and L_9, as shown in Fig. 1d. Figure 1a–d shows the process of the number of Lagrangian points increasing from eight to ten with increasing μ value.

In Fig. 2, we present the positional evolution of the Lagrangian points as the parameter q_1, given $\mu = 0.019$, $\sigma = 0.05, \gamma = 0.4, \alpha = 0.6, k = 0.00015$, $q_2 = q_3 = 0.9985$. In this case, there are eight non-collinear points, and all Lagrangian points are not symmetric about the u-axis. When q_1 increases at (0.6,1), the Lagrangian points L_1, L_2, L_7, and L_8 move away from the bigger primary m_1 in Fig. 2a. L_3 moves

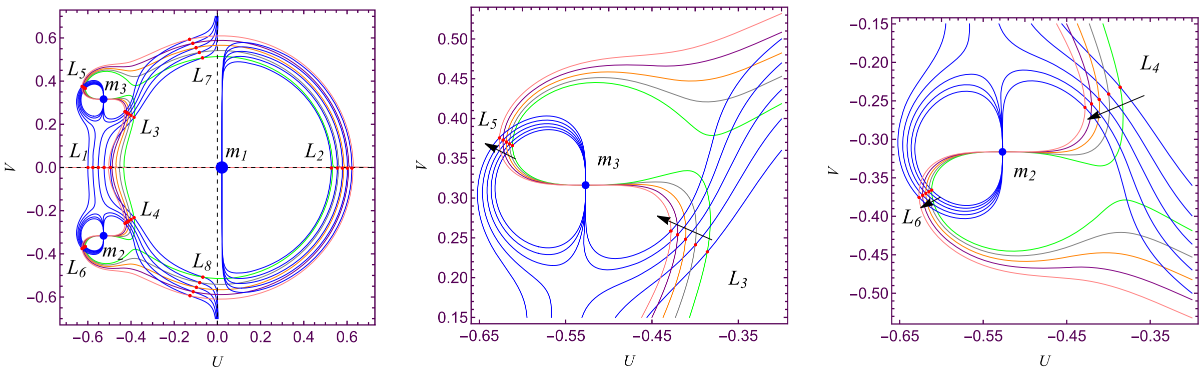

(a) Values range of q is $0.6 \le q_1 \le 1$

(b) Zoomed part of Figure 2(a) near primary m_3

(c) Zoomed part of Figure 2(a) near primary m_2

Fig. 2 The positions of Lagrangian points for $\mu = 0.019$, $\gamma = 0.4$, $\alpha = 0.6$, $\sigma = 0.05$, $k = 0.00015$, $q_2 = q_3 = 0.9985$, for different q_1 values, $q_1 = 0.6$ (blue, green), $q_1 = 0.7$ (blue, gray), $q_1 = 0.8$ (blue, orange), $q_1 = 0.9$ (blue, purple), $q_1 = 1$ (blue, pink). (Color figure online)

Fig. 3 The positions of Lagrangian points for $\mu = 0.01$, $\gamma = 0.6$, $\alpha = 0.4$, $\sigma = 0.05$, $k = 0.00001$, $q_2 = 0.8$, $q_3 = 0.6$, $q_1 = 0.6$ (blue, green), $q_1 = 0.7$ (blue, gray), $q_1 = 0.8$ (blue, orange), $q_1 = 0.9$ (blue, purple), $q_1 = 1$ (blue, pink). (Color figure online)

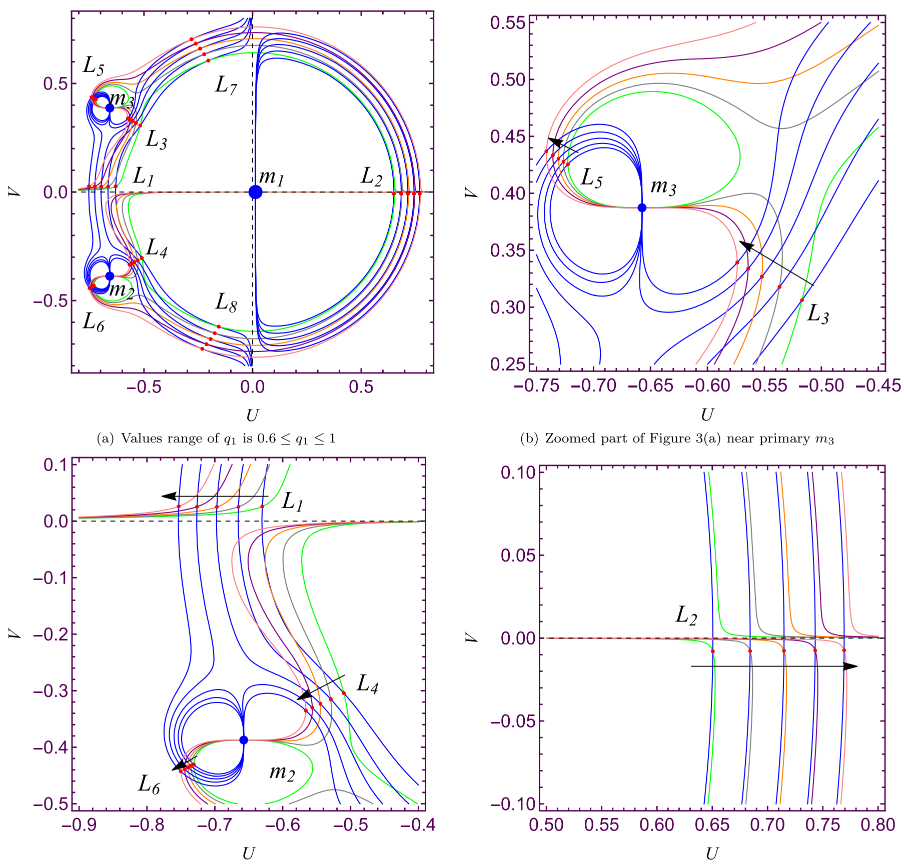

(a) Values range of q_1 is $0.6 \le q_1 \le 1$

(b) Zoomed part of Figure 3(a) near primary m_3

(c) Zoomed part of Figure 3(a) near primary m_2

(d) Zoomed part of Figure 3(a) near point L_2

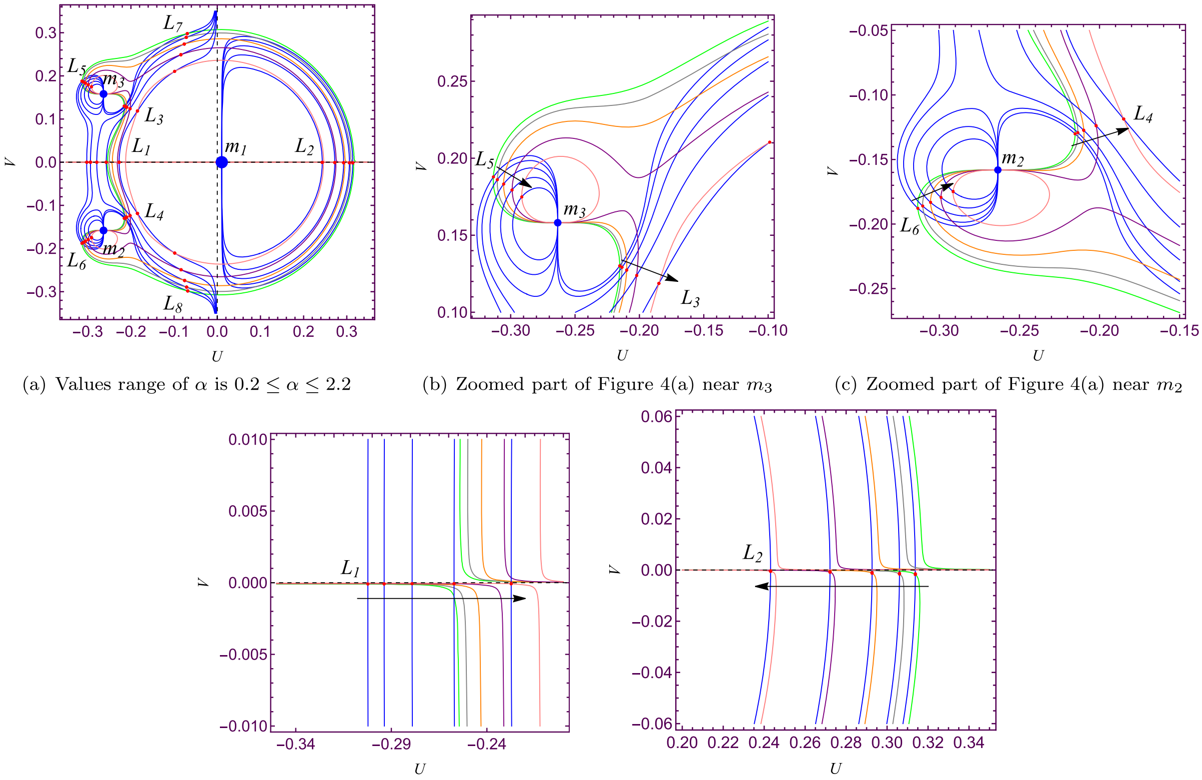

(a) Values range of α is $0.2 \le \alpha \le 2.2$

(b) Zoomed part of Figure 4(a) near m_3

(c) Zoomed part of Figure 4(a) near m_2

(d) Zoomed part of Figure 4(a) near point L_1

(e) Zoomed part of Figure 4(a) near point L_2

Fig. 4 The positions of Lagrangian points for $\mu = 0.019$, $\gamma = 0.1$, $\sigma = 0.05$, $q_1 = 0.95$, $q_2 = 0.9$, $q_3 = 0.9$, $k = 0.00015$, $\alpha = 0.2$ (blue, green), $\alpha = 0.6$ (blue, gray), $\alpha = 1$ (blue, orange), $\alpha = 1.5$ (blue, purple), $\alpha = 2.2$ (blue, pink). (Color figure online)

towards m_3 and L_5 moves away from m_3 in Fig. 2b. L_4 moves towards m_2 and L_6 moves away from m_2 in Fig. 2c. In addition, we also investigate the case of primaries m_2 and m_3 having different radiation effects ($q_2 \neq q_3$), and the Lagrangian points under the conditions are shown in Fig. 3. When q_1 increases at (0,1) and fixed parameters of $\mu = 0.01$, $\gamma = 0.6$, $\alpha = 0.4$, $\sigma = 0.05$, $k = 0.00001$, $q_2 = 0.8$, $q_3 = 0.6$, the Lagrangian points undergo a similar change in Fig. 3a–d.

The evolution of Lagrangian points is studied when $\mu = 0.019$, $\sigma = 0.05$, $\gamma = 0.1$, $q_1 = 0.95$, $q_2 = 0.9$, $q_3 = 0.9$, $k = 0.00015$, and α increases at (0.2,2.2) in Fig. 4. It can be observed that eight non-collinear points appear at this parameter value. As the α increases, all Lagrangian points move towards the origin, and the point L_3 moves toward m_3 and L_5 moves away from m_3 in Fig. 4b. L_4 moves towards m_2 and L_6 moves away from m_2, as shown in Fig. 4c. The Lagrangian points L_1 and L_2 move toward the primary m_1 on both sides of the origin near the u-axis in Fig. 4d–e, respectively.

In Fig. 5, the Lagrangian points are identified under the effect of k variation, with fixed values for $\mu = 0.019$, $\sigma = 0.05$, $\gamma = 0.12$, $\alpha = 0.19$, $q_1 = 0.99$, $q_2 = 0.98$, $q_3 = 0.98$ and $k \in (0.05, 0.4)$, six non-collinear points were found, and as the value of k increases, L_1 moves away from the primary m_3 and upwards to the left, L_3 moves away from primary m_3 and upwards to the right. L_5 moves towards primary m_3 and downwards to the left. These three Lagrangian points tend to merge. L_2 moves downwards to the primary m_2, while L_4 and L_6 move away from primary m_2 and upwards to the right and left, respectively. These three Lagrangian points also tend to merge.

4 Linear stability analysis of the Lagrangian points

Only the Lagrangian points around which an infinitesimal body can maintain motion are stable. Otherwise, it is unstable. Here, we have referred to the literature in [14]. If the coordinates of the Lagrangian points are (u_0, v_0), and (x, y) is the small displacement relative to the Lagrangian point, then this small displacement can be written as $x = u - u_0$, $y = v - v_0$. We expand the right-hand side of Eq. (8) to first-order by Taylor series, then Eq. (8) can be linearized to the following system

$$\begin{aligned}\ddot{x} - 2\dot{y} &= (S_{uu} + \Omega_{uu})_0\, x + (S_{uv} + \Omega_{uv})_0\, y - k\dot{x},\\ \ddot{y} + 2\dot{x} &= (S_{vu} + \Omega_{vu})_0\, x + (S_{vv} + \Omega_{vv})_0\, y - k\dot{y},\end{aligned} \tag{16}$$

where, subscript (0) represents the partial derivative at the Lagrangian point, let $(S_{uu} + \Omega_{uu})_0 = N_1$, $(S_{uv} + \Omega_{uv})_0 = N_2$, $(S_{vu} + \Omega_{vu})_0 = F_1$, $(S_{vv} + \Omega_{vv})_0 = F_2$ in "Appendix I". For the problem of variable mass, the location of the primary will change over time t, and their distances to the Lagrangian point (u_0, v_0) decrease with time t. Therefore, conventional methods cannot determine linear stability.That is why we have used Meshcherskii space time transformations $u = X\gamma^{\frac{1}{2}}, v = Y\gamma^{\frac{1}{2}}$. This fixes the positions of the primaries and the distance to the Lagrangian point. Let $\dot{x} = x_1$, $\dot{y} = y_1$, Eq. (16) in phase-space as

$$\begin{aligned}\dot{x_1} - 2y_1 &= (S_{uu} + \Omega_{uu})_0\, x + (S_{uv} + \Omega_{uv})_0\, y - kx_1,\\ \dot{y_1} + 2x_1 &= (S_{vu} + \Omega_{vu})_0\, x + (S_{vv} + \Omega_{vv})_0\, y - ky_1.\end{aligned} \tag{17}$$

Consider the Meshcherskii inverse transform, and take $X' = \gamma^{-1/2}x, Y' = \gamma^{-1/2}y, x' = \gamma^{-1/2}x_1, y' = \gamma^{-1/2}y_1$. The Eq. (17) can be rewritten as the matrix form

$$\begin{bmatrix} \frac{dX'}{dt} \\ \frac{dY'}{dt} \\ \frac{dx'}{dt} \\ \frac{dy'}{dt} \end{bmatrix} = \begin{bmatrix} \frac{\alpha}{2} & 0 & 1 & 0 \\ 0 & \frac{\alpha}{2} & 0 & 1 \\ N_1 & N_2 & \frac{\alpha}{2} - k & 2 \\ F_1 & F_2 & -2 & \frac{\alpha}{2} - k \end{bmatrix} \begin{bmatrix} X' \\ Y' \\ x' \\ y' \end{bmatrix}. \tag{18}$$

The linear stability of Eqs. (8) and (18) is consistent with each other. We determine the linear stability of the Lagrangian points by solving the eigenvalues of the coefficient matrix of Eq. (18) numerically. The characteristic equation of the linearized Eq. (18) corresponding to the equilibrium point is

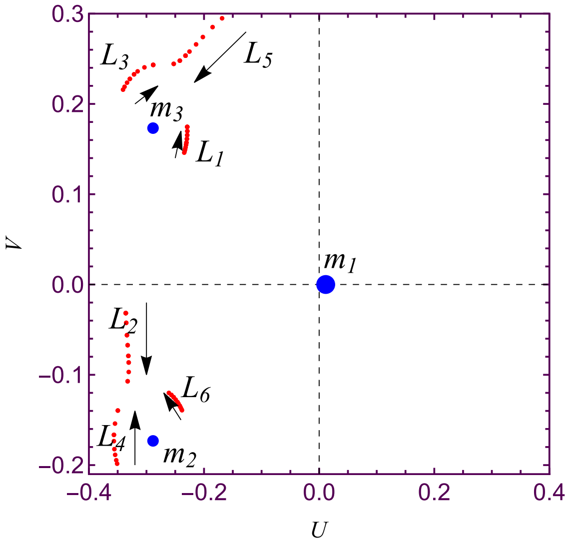

Fig. 5 The positions of Lagrangian points for $\mu = 0.019$, $\gamma = 0.12$, $\alpha = 0.19$, $\sigma = 0.05$, $q_1 = 0.99$, $q_2 = 0.98$, $q_3 = 0.98$ when $0.05 \le k \le 0.4$.

$$\begin{aligned}&\lambda^4 + 2(k-\alpha)\lambda^3 + \left[f_1 + \frac{1}{2}(3\alpha)(\alpha - 2k)\right]\lambda^2\\ &-\left[\alpha f_1 + f_2 - \frac{1}{2}\left(3\alpha^2\right)(k-\alpha)\right]\lambda\\ &+\frac{\alpha^4}{16} - \frac{1}{4}\left(\alpha^3 k\right)\\ &+\frac{\alpha^2 f_1}{4} + \frac{\alpha f_2}{2} + f_3 = 0,\end{aligned} \tag{19}$$

where

$$\begin{aligned}f_1 &= -F_2 + k^2 - N_1 + 4,\\ f_2 &= k\,(F_2 + N_1) + 2F_1 - 2N_2,\\ f_3 &= F_2 N_1 - N_2 F_1.\end{aligned} \tag{20}$$

If four complex roots of the characteristic Eq. (19) all have negative real parts or are pure imaginary roots, then the corresponding Lagrangian point is asymptotically stable or stable. If there are roots with positive real parts, it is unstable. Under the influence of photo-gravitational, variable mass, and Stokes drag, all Lagrangian points are unstable.

5 Zero-velocity curves

This section studies the zero-velocity curve of the variable mass R4BP under the perturbation of photo-gravitational and Stokes drag. The expression for the possible motion region of the fourth body is

$$\begin{aligned} (\Omega+S)(\gamma) &\geq C(\gamma) \quad \text{for} \quad \frac{\partial}{\partial\gamma}(\Omega+S) \geqslant 0, \\ (\Omega+S)(\gamma_0) &\geq C(\gamma_0) \quad \text{for} \quad \frac{\partial}{\partial\gamma}(\Omega+S) \leqslant 0, \end{aligned} \tag{21}$$

where

$$C(\gamma) = -\frac{V_0^2}{2} + S + \Omega(\gamma, u_0, v_0), \; V_0^2 = u_0^2 + v_0^2 \tag{22}$$

Using the obtained relation in Eq. (12), these curves can be identified by

$$2(S+\Omega) - C - 2\int_0^t \frac{\partial}{\partial t}(S+\Omega)dt > 0. \tag{23}$$

In Fig. 6, we plot the zero-velocity curve under the Jacobian constant C value variation for fixed parameters $\mu = 0.019$, $\alpha = 0.4$, $\gamma = 0.3$, $k = 0.00015$, $q_1 = 0.9$, $q_2 = q_3 = 0.8$. The blue and red dots denote the primaries and Lagrangian points, respectively. The yellow and white regions represent the Hill and forbidden regions, respectively. The Hill region refers to the region where infinitesimal body may move, and the forbidden region is the region where the infinitesimal body cannot reach. In Fig. 6, there are eight non-collinear Lagrangian points, all of which are not symmetric about the u-axis.

In Fig. 6a, the Jacobian integral C=0.456375 and the Lagrangian points L_1, L_2, L_7, and L_8 are all located in the forbidden region. The infinitesimal body cannot reach these Lagrangian points, while L_3, L_4, L_5, and L_6 are located in the Hill region. Especially, L_3 and L_4 are trapped in the Hill region with the primaries m_3 and m_2, respectively. This means the infinitesimal body cannot travel from one primary to another. In Fig. 6b, the Jacobian integral C decreases to 0.454533. It can be observed that there is a gap between L_3 and L_5, L_4 and L_6, and the infinitesimal body can reach either L_5 or L_6 from m_3 and m_2. In Fig. 6c, the Jacobian integral constant C decreases to 0.442488, and two branches appear near the primaries m_3 and m_2. That infinitesimal body can freely move between the primaries, but L_1, L_2, L_7, and L_8 are still trapped in the forbidden zone. In Fig. 6d, C decreases to 0.426496, and all Lagrangian points are located in the Hill region, but forbidden regions block L_1, L_7, and L_8. In Fig. 6e, f, Jacobian integral C decreases to 0.422425 and 0.420288, respectively. The forbidden regions near L_1 disappear first, and then the forbidden regions around L_7 and L_8 disappear. All Lagrangian points are located in the Hill region, meaning the infinitesimal body can shuttle between all primary bodies and all Lagrangian points.

6 Periodic solutions near the non-collinear points

In the framework of R4BP with variable mass, the study of motion near the Lagrangian points is significant. Periodic solutions near unstable non-collinear Lagrangian points can allow the fourth body to maintain longer periods here. The LP method used to remove secular terms and provides periodic solutions for regular motion. A brief introduction of this method can be found in "Appendix II".

Move the $-k\dot{u}$ and $-k\dot{v}$ term in the stokes force on the right side of Eq. (8) to the left side then this equation can be rewritten as

$$\begin{aligned} \ddot{u} - 2\dot{v} + k\dot{u} &= \Omega_u + S_u^*, \\ \ddot{v} + 2\dot{u} + k\dot{v} &= \Omega_v + S_v^*, \end{aligned} \tag{24}$$

where

$$\begin{aligned} S_u^* &= -k\left[\frac{\alpha u}{2} - v\left(1 + \frac{3\gamma^{7/4}\sigma}{2\left(u^2+v^2\right)^{7/4}}\right)\right], \\ S_v^* &= -k\left[\frac{\alpha v}{2} + u\left(1 + \frac{3\gamma^{7/4}\sigma}{2\left(u^2+v^2\right)^{7/4}}\right)\right]. \end{aligned} \tag{25}$$

Introducing transformations $u = u_0 + x$, $v = v_0 + y$, then Eq. (24) become the following form

$$\begin{aligned} \ddot{x} - 2\dot{y} + k\dot{x} &= \Omega_x + S_x^*, \\ \ddot{y} + 2\dot{x} + k\dot{y} &= \Omega_y + S_y^*. \end{aligned} \tag{26}$$

Utilizing Eq. (26) and applying the Taylor series up to third-order term, we get

$$\begin{aligned} \ddot{x} - 2\dot{y} + k\dot{x} = U_x^0 &+ U_x^0\left(x\frac{\partial}{\partial x} + y\frac{\partial}{\partial y}\right) \\ &+ \frac{1}{2!}U_x^0\left(x\frac{\partial}{\partial x} + y\frac{\partial}{\partial y}\right)^2 \\ &+ U_x^0\frac{1}{3!}\left(x\frac{\partial}{\partial x} + y\frac{\partial}{\partial y}\right)^3 + O(4), \\ \ddot{y} + 2\dot{x} + k\dot{y} = U_y^0 &+ U_y^0\left(x\frac{\partial}{\partial x} + y\frac{\partial}{\partial y}\right) \end{aligned}$$

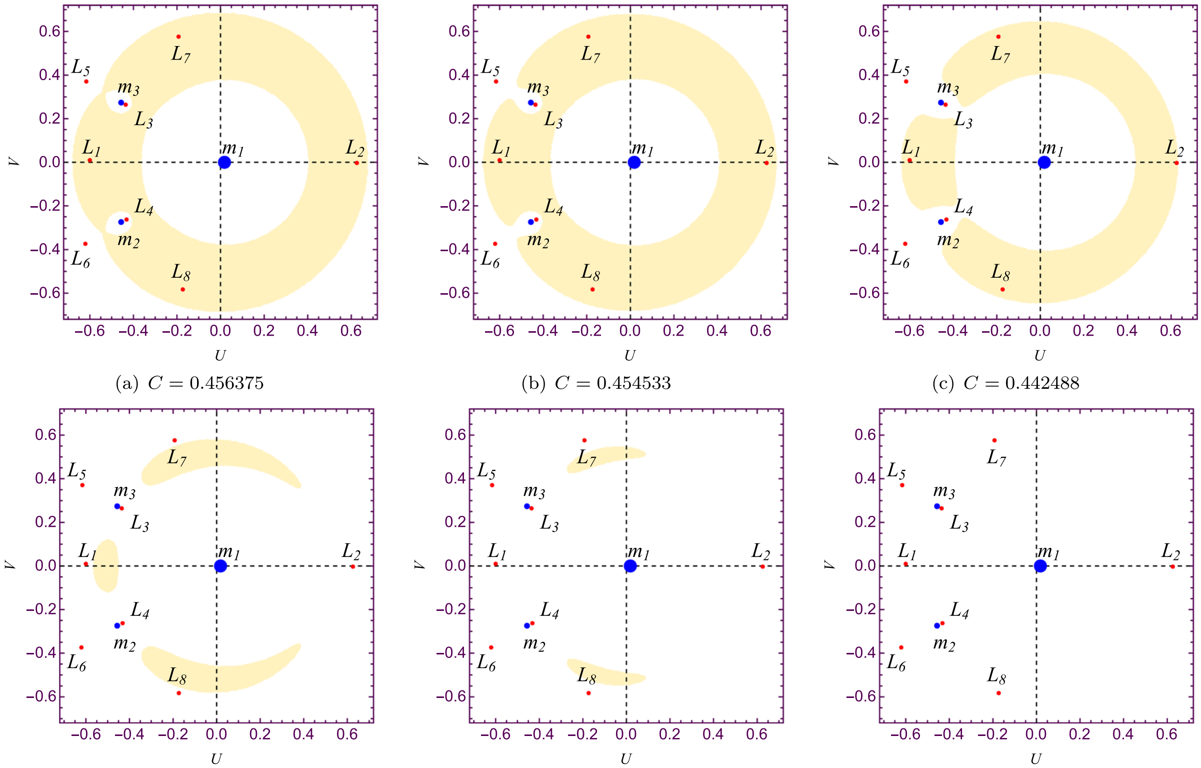

(a) $C = 0.456375$ (b) $C = 0.454533$ (c) $C = 0.442488$

(d) $C = 0.426496$ (e) $C = 0.422425$ (f) $C = 0.420288$

Fig. 6 The zero-velocity curve in the R4BP with the photo-gravitational, variable mass, and Stokes drag perturbations for $\mu = 0.019,\ \alpha = 0.4,\ k = 0.00015,\ \gamma = 0.3,\ q_1 = 0.9,\ q_2 = q_3 = 0.8$, for different C values

$$+\frac{1}{2!}U_y^0\left(x\frac{\partial}{\partial x}+y\frac{\partial}{\partial y}\right)^2 + U_y^0\frac{1}{3!}\left(x\frac{\partial}{\partial x}+y\frac{\partial}{\partial y}\right)^3 + O(4), \tag{27}$$

where $U_x = \Omega_x + S_x^*$, the superscript $(^0)$ represents the value evaluated at the Lagrangian point, $O(4)$ represents fourth-order and higher-order terms, which we ignore here. At the Lagrangian points $L_i, i = 1, 2, \cdots, 10,\ U_x^0(L_i) = U_y^0(L_i) = 0$. Therefore, the equation can be further expanded and simplified as

$$\begin{aligned}\ddot{x} - 2\dot{y} + k\dot{x} = {}& U_{xx}^0 x + U_{xy}^0 y + \frac{1}{2}U_{xxx}^0 x^2 \\ &+ U_{xxy}^0 xy + \frac{1}{2}U_{xyy}^0 y^2 \\ &+ \frac{1}{6}U_{xxxx}^0 x^3 + \frac{1}{2}U_{xxxy}^0 x^2 y \\ &+ \frac{1}{2}U_{xxyy}^0 xy^2 + \frac{1}{6}U_{xyyy}^0 y^3, \\ \ddot{y} + 2\dot{x} + k\dot{y} = {}& U_{yx}^0 x + U_{yy}^0 y + \frac{1}{2}U_{yxx}^0 x^2 \\ &+ U_{yxy}^0 xy + \frac{1}{2}U_{yyy}^0 y^2 \\ &+ \frac{1}{6}U_{yxxx}^0 x^3 + \frac{1}{2}U_{yxxy}^0 x^2 y \\ &+ \frac{1}{2}U_{yxyy}^0 xy^2 + \frac{1}{6}U_{yyyy}^0 y^3,\end{aligned} \tag{28}$$

where $U_{xx}^0 = N_1$, $U_{xy}^0 = N_2$, $U_{xxx}^0 = 2N_3$, $U_{xxy}^0 = N_4$, $U_{xyy}^0 = 2N_5$, $U_{xxxx}^0 = 6N_6$, $U_{xxxy}^0 = 2N_7$, $U_{xxyy}^0 = 2N_8$, $U_{xyyy}^0 = 6N_9$, $U_{yx}^0 = F_1$, $U_{yy}^0 = F_2$, $U_{yxx}^0 = 2F_3$, $U_{yxy}^0 = F_4$, $U_{yyy}^0 = 2F_5$, $U_{yxxx}^0 = 6F_6$, $U_{yxxy}^0 = 2F_7$, $U_{yxyy}^0 = 2F_8$, $U_{yyyy}^0 = 6F_9$, and $N_i, i = 1, 2, \ldots, 9$, $F_i, i = 1, 2, \ldots, 9$ in "Appendix I".

The coefficients are represented by $N_i, F_i, i = 1, 2, \ldots, 9$, and the Eq. (28) can be rewritten as

$$\begin{aligned}\ddot{x} - 2\dot{y} + k\dot{x} &= N_1 x + N_2 y + N_3 x^2 + N_4 xy + N_5 y^2 \\ &\quad + N_6 x^3 + N_7 x^2 y + N_8 xy^2 + N_9 y^3, \\ \ddot{y} + 2\dot{x} + k\dot{y} &= F_1 x + F_2 y + F_3 x^2 + F_4 xy + F_5 y^2 \\ &\quad + F_6 x^3 + F_7 x^2 y + F_8 xy^2 + F_9 y^3.\end{aligned} \tag{29}$$

Supposing that the form of the solution to Eq. (29) is

$$\begin{aligned} x &= x_1\epsilon + x_2\epsilon^2 + x_3\epsilon^3, \\ y &= y_1\epsilon + y_2\epsilon^2 + y_3\epsilon^3, \end{aligned} \tag{30}$$

where ϵ is a small parameter and value range is $|\epsilon| \ll 1$. Substituting Eqs. (30) into (29) and comparing the powers of ϵ on both sides. Thus, we obtain the following three linear systems concerning the coefficients of ϵ, ϵ^2, and ϵ^3 in the following forms

$$\begin{aligned} \ddot{x}_1 - 2\dot{y}_1 + k\dot{x}_1 &= N_1 x + N_2 y_1, \\ \ddot{y}_1 + 2\dot{x}_1 + k\dot{y}_1 &= F_1 x_1 + F_2 y_1, \end{aligned} \tag{31}$$

$$\begin{aligned} \ddot{x}_2 - 2\dot{y}_2 + k\dot{x}_2 &= N_1 x_2 + N_2 y_2 + N_3 x_1^2 \\ &\quad + N_4 x_1 y_1 + N_5 y_1^2, \\ \ddot{y}_2 + 2\dot{x}_2 + k\dot{y}_2 &= F_1 x_2 + F_2 y_2 + F_3 x_1^2 \\ &\quad + F_4 x_1 y_1 + F_5 y_1^2. \end{aligned} \tag{32}$$

$$\begin{aligned} \ddot{x}_3 - 2\dot{y}_3 + k\dot{x}_3 &= N_1 x_3 + N_2 y_3 + 2N_3 x_1 x_2 \\ &\quad + N_4 x_1 y_2 + N_4 x_2 y_1 + 2N_5 y_1 y_2 \\ &\quad + N_6 x_1^3 + N_7 x_1^2 y_1 \\ &\quad + N_8 x_1 y_1^2 + N_9 y_1^3, \\ \ddot{y}_3 + 2\dot{x}_3 + k\dot{y}_3 &= F_1 x_3 + F_2 y_3 + 2F_3 x_1 x_2 \\ &\quad + F_4 x_1 y_2 + F_4 x_2 y_1 + 2F_5 y_1 y_2 \\ &\quad + F_6 x_1^3 + F_7 x_1^2 y_1 \\ &\quad + F_8 x_1 y_1^2 + F_9 y_1^3. \end{aligned} \tag{33}$$

For the Eq. (31), supposing that the form of the solutions are

$$\begin{aligned} x_1 &= G_1 \cos(\omega t) + H_1 \sin(\omega t), \\ y_1 &= G_2 \cos(\omega t) + H_2 \sin(\omega t), \end{aligned} \tag{34}$$

where period $T = 2\pi/\omega$.
Substituting Eq. (34) into (31) yields

$$\begin{aligned} A_{11}\ \sin(\omega t) + B_{11}\ \cos(\omega t) &= 0, \\ A_{21}\ \sin(\omega t) + B_{21}\ \cos(\omega t) &= 0, \end{aligned} \tag{35}$$

where

$$\begin{aligned} A_{11} &= \left[2G_1\omega + G_2 k\omega + F_1 H_1 + \left(F_2 + \omega^2\right) H_2\right], \\ B_{11} &= \left[F_1 G_1 + \left(F_2 + \omega^2\right) G_2 - 2H_1\omega - H_2 k\omega\right], \\ A_{21} &= \left[G_1 k\omega - 2G_2\omega + H_1\left(N_1 + \omega^2\right) + H_2 N_2\right], \\ B_{21} &= \left[G_1\left(N_1 + \omega^2\right) + G_2 N_2 - H_1 k\omega + 2H_2\omega\right]. \end{aligned} \tag{36}$$

In order to make the homogeneous system of Eq. (35) have non-zero solutions, the determinant is zero, as follows

$$\begin{vmatrix} N_1 + \omega^2 & N_2 & -k\,\omega & 2\,\omega \\ k\,\omega & -2\,\omega & N_1 + \omega^2 & N_2 \\ F_1 & F_2 + \omega^2 & -2\,\omega & -k\,\omega \\ 2\,\omega & k\,\omega & F_1 & F_2 + \omega^2 \end{vmatrix} = 0. \tag{37}$$

Set $H_2 = 1$, obtain G_1, G_2, H_1 in "Appendix III". So the solutions of Eq. (31) are

$$\begin{aligned} x_1 &= G_1 \cos(\omega t) + H_1 \sin(\omega t), \\ y_1 &= G_2 \cos(\omega t) + \sin(\omega t). \end{aligned} \tag{38}$$

Similarly, to solve Eq. (32), let the solutions take the form of

$$\begin{aligned} x_2 &= G_3 \cos(\omega t) + G_4 \cos(2\omega t) \\ &\quad + H_3 \sin(\omega t) + H_4 \sin(2\omega t), \\ y_2 &= G_5 \cos(\omega t) + G_6 \cos(2\omega t) \\ &\quad + H_5 \sin(\omega t) + H_6 \sin(2\omega t). \end{aligned} \tag{39}$$

By using the same method as solving Eq. (31) and substituting the already obtained (x_1, y_1) in Eq. (38) into (32), we obtain $G_3 = 0$, $H_3 = 0$, $G_5 = 0$, $H_5 = 0$, and G_4, G_6, H_4, H_6 in "Appendix III". Therefore, the solutions of Eq. (32) are given by

$$\begin{aligned} x_2 &= G_4 \cos(2\omega t) + H_4 \sin(2\omega t), \\ y_2 &= G_6 \cos(2\omega t) + H_6 \sin(2\omega t). \end{aligned} \tag{40}$$

So, the second-order periodic solution is

$$\begin{aligned} x &= \epsilon\left[G_1 \cos(\omega t) + H_1 \sin(\omega t)\right] \\ &\quad + \epsilon^2\left[G_4 \cos(2\omega t) + H_4 \sin(2\omega t)\right], \\ y &= \epsilon\left[G_2 \cos(\omega t) + \sin(\omega t)\right] \\ &\quad + \epsilon^2\left[G_6 \cos(2\omega t) + H_6 \sin(2\omega t)\right]. \end{aligned} \tag{41}$$

Similarly, to solve Eq. (33), let the solutions take the below forms

$$\begin{aligned} x_3 &= G_7 \cos(\omega t) + G_8 \cos(2\omega t) + G_9 \cos(3\omega t) \\ &\quad + H_7 \sin(\omega t) + H_8 \sin(2\omega t) + H_9 \sin(3\omega t), \\ y_3 &= G_{10} \cos(\omega t) + G_{11} \cos(2\omega t) + G_{12} \cos(3\omega t) \\ &\quad + H_{10} \sin(\omega t) + H_{11} \sin(2\omega t) + H_{12} \sin(3\omega t). \end{aligned} \tag{42}$$

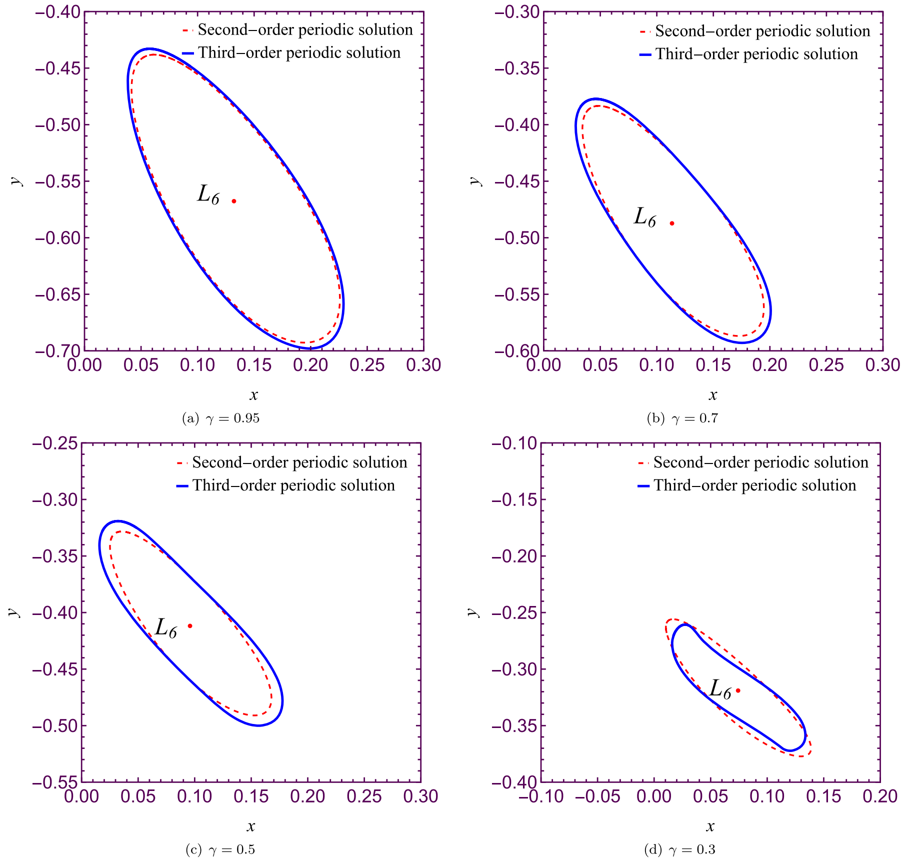

Fig. 7 Second- and third-order periodic solutions, for fixed parameter $\mu = 0.25$, $\sigma = 0.05$, $k = 0.00005$, $q_1 = 0.99$, $q_2 = 0.9985$, $q_3 = 0.9985$, $\alpha = 2.2$ at different values for mass variation parameter. The second-order periodic solution is represented by the red dotted line, while the third-order periodic solution is depicted by the thick blue line. (Color figure online)

By using the same method as above and substituting the already obtained (x_1, y_1) and (x_2, y_2) in Eqs. (38, 40) into Eq. (33), we obtain $G_8 = 0$, $G_{11} = 0$, $H_7 = 0$, $H_8 = 0$, $H_{11} = 0$, $H_{12} = 1$, and G_7, G_9, G_{10}, G_{12}, H_9, H_{12} in “Appendix III”. Therefore, the solutions to Eq. (33) are

$$\begin{aligned} x_3 &= G_7\cos(\omega t) + G_9\cos(3\omega t) + H_9\sin(3\omega t), \\ y_3 &= G_{10}\cos(\omega t) + G_{12}\cos(3\omega t) \\ &\quad + H_{10}\sin(\omega t) + \sin(3\omega t). \end{aligned} \tag{43}$$

So, the third-order periodic solution is

$$\begin{aligned} x &= \epsilon\,[G_1\cos(\omega t) + H_1\sin(\omega t)] \\ &\quad + \epsilon^2\,[G_4\cos(2\omega t) + H_4\sin(2\omega t)] \\ &\quad + \epsilon^3\,[G_7\cos(\omega t) + G_9\cos(3\omega t) + H_9\sin(3\omega t)], \\ y &= \epsilon\,[G_2\cos(\omega t) + \sin(\omega t)] \\ &\quad + \epsilon^2\,[G_6\cos(2\omega t) + H_6\sin(2\omega t)] \\ &\quad + \epsilon^3\,[G_{10}\cos(\omega t) + G_{12}\cos(3\omega t) \\ &\quad + H_{10}\sin(\omega t) + \sin(3\omega t)]\,. \end{aligned} \tag{44}$$

Fixed the parameter $\mu = 0.25$, $\sigma = 0.05$, $k = 0.00005$, $q_1 = 0.99$, $q_2 = 0.9985$, $q_3 = 0.9985$, $\alpha = 2.2$, when $\gamma = 0.95, 0.7, 0.5, 0.3$, the coordinates of Lagrangian points $L_6 = (0.132165, -0.567669)$, $(0.113444, -0.487284)$, $(0.0958778, -0.41183)$ and $(0.0742666, -0.319002)$ are obtained respectively. The corresponding second- and third-order periodic solutions are shown in Fig. 7a–d, respectively. When γ has a larger value of 0.95, it can be observed that the second- and third-order periodic solutions of the non-collinear Lagrangian point L_6 are very close, and in some areas they are close to overlapping. When γ decreases to 0.7, the difference between the second- and third-order periodic solutions at point L_6 increases. When γ decreases to 0.5, the difference between the second- and third-order periodic solutions increases, and both become somewhat flatter. When γ decreases to 0.3, in addition to the above changes, the third-order periodic solution no longer resembles a smooth ellipse and undergoes significant deformation. Furthermore, as γ decreases, the coordinates of Lagrangian point L_6 approach the origin and the periodic solution shrinks constantly.

7 Conclusions

The equations of motion were obtained for the R4BP with variable mass under the perturbations of photo-gravitational and Stokes forces. The Lagrangian points were calculated with parameters $0 < \mu \leq 1/3$, $0 < \alpha \leq 2.2$, $\sigma, k, \gamma \in (0, 1)$, $0 < q_i \leq 1$ $(i = 1, 2, 3)$ and found that under the joint perturbation of photo-gravitational, Stokes force, and variable mass, there are six, eight, or ten non-collinear Lagrangian points, and there are no collinear Lagrangian points.

As the radiation pressure q_1 of the primary body m_1 increases in (0.6,1), the Lagrangian points are all far from the origin, while for the primary bodies, the Lagrangian points are either closer or farther away from it, regardless of whether the radiation of the second- and third primary bodies are equal. When the dissipative force constant $k \in (0.05, 0.4)$, there are six Lagrangian points, and with the increase of k value, these points are divided into L_1, L_3, L_5, and L_2, L_4, L_6, two groups, and the points in each group are closer and closer. As the variable mass parameter varies in (0.2,2.2), the coordinates of the Lagrangian points all move toward the origin. For different primary bodies, the Lagrangian points near them tend to move away or close to them. Through linear stability calculations, it was found that all Lagrangian points under the parameters considered in this paper are unstable.

Through the zero-velocity curves plotted for the given parameters, it is found that when the Jacobian integral constant changes within the range of (0.456375, 0.420288), the zero-velocity surface also changes, the Hill region gradually increases, and it is possible to transition between the primaries. With the help of the LP method, we also present the second- and third-order analytical periodic solutions around the non-collinear Lagrangian point. The numerical simulation results near the point L_6 show that a substantial increase in the mass change parameter γ results in a larger area surrounding the periodic solution of L_6, exhibiting a visually regular elliptical shape. Conversely, a decrease in γ leads to a reduction in the region of periodic solutions, accompanied by notable alterations in shape, particularly concerning third-order periodic solutions.

Acknowledgements We are very grateful to the anonymous reviewers whose comments and suggestions helped improve and clarify this paper. The second author, therefore, acknowledges his gratitude for NRIAG's technical and financial support.

Author contributions Formal analysis: B. Ma, E. I. Abouelmagd, F.B. Gao; Investigation: B. Ma, E. I. Abouelmagd, F.B. Gao; Methodology: B. Ma, E. I. Abouelmagd, F.B. Gao; Project administration: E. I. Abouelmagd, F.B. Gao; Software: B. Ma, E. I. Abouelmagd, F.B. Gao; Validation: B. Ma, E. I. Abouelmagd, F.B. Gao; Visualization: B. Ma, E. I. Abouelmagd, F.B. Gao; Writing–original draft: B. Ma, E. I. Abouelmagd; Writing–review and editing: B. Ma, E. I. Abouelmagd, F.B. Gao; Approval of the version of the manuscript to be published: B. Ma, E. I. Abouelmagd, F.B. Gao.

Funding This research was funded by the National Natural Science Foundation of China (NSFC) through Grant No. 12172322, and the "High-end Talent Support Program" of Yangzhou University, China. Moreover, this paper was also supported by the National Research Institute of Astronomy and Geophysics (NRIAG), Helwan 11421, Cairo, Egypt.

Data availability The study does not report any data.

Declaration

Conflict of interest The authors declare no Conflict of interest.

Appendix I

$$
\begin{aligned}
N_1 =& \frac{1}{4}\left[\gamma^{3/2}\left(\frac{4(2\mu-1)q_1(r_1^2-3J_1^2)}{r_1^5}+12J_2^2\mu\left(\frac{q_2}{r_2^5}+\frac{q_3}{r_3^5}\right)\right.\right.\\
&\left.\left.-\frac{21\sqrt[4]{\gamma}k\sigma u_0 v_0}{r_0^{11/2}}-\frac{4\mu q_2}{r_2^3}+\frac{4\mu q_3}{r_3^3}\right)+\alpha^2-2\alpha k+4\right],\\
N_2 =& 3\gamma^{3/2}\left[J_2^2\left(-\frac{5J_3\mu q_2}{r_2^7}-\frac{5J_4\mu q_3}{r_3^7}\right)+\frac{J_3\mu q_2}{r_2^5}+\frac{J_4\mu q_3}{r_3^5}-\frac{(2\mu-1)q_1 v_0(r_1^2-5J_1^2)}{r_1^7}\right]\\
&+\frac{21\gamma^{7/4}k\sigma u_0(11v_0^2-2r_0^2)}{8r_0^{15/2}},\\
N_3 =& \frac{3}{16}\gamma^{3/2}\left[8\left(5J_2^3\mu\left(-\frac{q_2}{r_2^7}-\frac{q_3}{r_3^7}\right)+3J_2\mu\left(\frac{q_2}{r_2^5}+\frac{q_3}{r_3^5}\right)+\frac{J_1(2\mu-1)q_1(5J_1^2-3r_1^2)}{r_1^7}\right)\right.\\
&\left.+\frac{7\sqrt[4]{\gamma}k\sigma v_0(11u_0^2-2r_0^2)}{r_0^{15/2}}\right],\\
N_4 =& 3\gamma^{3/2}\left[J_2^2\left(-\frac{5J_3\mu q_2}{r_2^7}-\frac{5J_4\mu q_3}{r_3^7}\right)+\frac{J_3\mu q_2}{r_2^5}+\frac{J_4\mu q_3}{r_3^5}-\frac{(2\mu-1)q_1 v_0(r_1^2-5J_1^2)}{r_1^7}\right]\\
&+\frac{21\gamma^{7/4}k\sigma u_0(11v_0^2-2r_0^2)}{8r_0^{15/2}},\\
N_5 =& \frac{1}{2}\left[\gamma^{3/2}\left(3J_2\mu\left(\frac{q_2\left(r_2^2-5J_3^2\right)}{r_2^7}+\frac{q_3\left(r_3^2-5J_4^2\right)}{r_3^7}\right)-\frac{3J_1(2\mu-1)q_1\left(r_1^2-5v_0^2\right)}{r_1^7}\right)\right.\\
&\left.+\frac{21\gamma^{7/4}k\sigma v_0\left(11v_0^2-6r_0^2\right)}{8r_0^{15/2}}\right],\\
N_6 =& \frac{1}{2}\gamma^{3/2}\left[\frac{35J_1^4(1-2\mu)q_1}{r_1^9}+\frac{30J_1^2(2\mu-1)q_1}{r_1^7}+\mu\left(35J_2^4\left(\frac{q_2}{r_2^9}+\frac{q_3}{r_3^9}\right)+J_2^2\left(-\frac{30q_2}{r_2^7}-\frac{30q_3}{r_3^7}\right)\right.\right.\\
&\left.\left.+\frac{3q_2}{r_2^5}+\frac{3q_3}{r_3^5}\right)+\frac{3(1-2\mu)q_1}{r_1^5}\right]+\frac{231\gamma^{7/4}k\sigma v_0\left(2r_0^2u_0-5u_0^3\right)}{32r_0^{19/2}},\\
N_7 =& \frac{3}{32}\gamma^{3/2}\left[80\left(\frac{7J_4J_2^3\mu q_3}{r_3^9}+\frac{J_3J_2\mu q_2\left(7J_2^2-3r_2^2\right)}{r_2^9}-\frac{3J_4J_2\mu q_3}{r_3^7}+\frac{J_1(2\mu-1)q_1 v_0\left(3r_1^2-7J_1^2\right)}{r_1^9}\right)\right.\\
&\left.-\frac{7\sqrt[4]{\gamma}k\sigma\left(-22r_0^2\left(u_0^2+v_0^2\right)+4r_0^4+165u_0^2v_0^2\right)}{r_0^{19/2}}\right],\\
N_8 =& \frac{3}{2}\gamma^{3/2}\left[\mu\left(\frac{35J_2^2J_4^2q_3}{r_3^9}+\frac{q_2\left(-5\left(J_2^2+J_3^2\right)r_2^2+35J_2^2J_3^2+r_2^4\right)}{r_2^9}-\frac{5\left(J_2^2+J_4^2\right)q_3}{r_3^7}+\frac{q_3}{r_3^5}\right)\right.\\
&\left.+\frac{5J_1^2(2\mu-1)q_1\left(r_1^2-7v_0^2\right)}{r_1^9}-\frac{(2\mu-1)q_1\left(r_1^2-5v_0^2\right)}{r_1^7}\right]+\frac{693\gamma^{7/4}k\sigma u_0\left(2r_0^2v_0-5v_0^3\right)}{32r_0^{19/2}},
\end{aligned}
$$

$$
\begin{aligned}
N_9 =&\frac{5}{2}\gamma^{3/2}\left[J_2\mu\left(\frac{q_2\left(7J_3^3-3J_3r_2^2\right)}{r_2^9}+\frac{q_3\left(7J_4^3-3J_4r_3^2\right)}{r_3^9}\right)+\frac{J_1(2\mu-1)q_1v_0\left(3r_1^2-7v_0^2\right)}{r_1^9}\right]\\
&-\frac{21\gamma^{7/4}k\sigma\left(-44r_0^2v_0^2+4r_0^4+55v_0^4\right)}{32r_0^{19/2}},\\
F_1 =&3\gamma^{3/2}\left[J_2\mu\left(\frac{J_3q_2}{r_2^5}+\frac{J_4q_3}{r_3^5}\right)+\frac{J_1(1-2\mu)q_1v_0}{r_1^5}\right]+\frac{1}{4}k\left[\frac{3\gamma^{7/4}\sigma\left(7u_0^2-2r_0^2\right)}{r_0^{11/2}}-4\right],\\
F_2 =&\gamma^{3/2}\left[-\frac{\mu q_2\left(r_2^2-3J_3^2\right)}{r_2^5}-\frac{\mu q_3\left(r_3^2-3J_4^2\right)}{r_3^5}+\frac{21\sqrt[4]{\gamma}k\sigma u_0v_0}{4r_0^{11/2}}+\frac{(2\mu-1)q_1\left(r_1^2-3v_0^2\right)}{r_1^5}\right]+\frac{\alpha^2-2\alpha k}{4}+1,\\
F_3 =&\frac{3}{16}\gamma^{3/2}\left[40J_2^2\mu\left(-\frac{J_3q_2}{r_2^7}-\frac{J_4q_3}{r_3^7}\right)+\frac{8J_3\mu q_2}{r_2^5}+\frac{8J_4\mu q_3}{r_3^5}-\frac{8(2\mu-1)q_1v_0\left(r_1^2-5J_1^2\right)}{r_1^7}\right.\\
&\left.+\frac{7\sqrt[4]{\gamma}k\sigma\left(6r_0^2u_0-11u_0^3\right)}{r_0^{15/2}}\right],\\
F_4 =&\gamma^{3/2}\left[3J_2\mu\left(\frac{q_2\left(r_2^2-5J_3^2\right)}{r_2^7}+\frac{q_3\left(r_3^2-5J_4^2\right)}{r_3^7}\right)-\frac{3J_1(2\mu-1)q_1\left(r_1^2-5v_0^2\right)}{r_1^7}\right]+\frac{21\gamma^{7/4}k\sigma v_0\left(2r_0^2-11u_0^2\right)}{8r_0^{15/2}},\\
F_5 =&\frac{3}{16}\gamma^{3/2}\left[8\left(-\frac{5J_3^3\mu q_2}{r_2^7}+\frac{3J_3\mu q_2}{r_2^5}+\frac{3J_4\mu q_3}{r_3^5}-\frac{5J_4^3\mu q_3}{r_3^7}+\frac{(2\mu-1)q_1v_0\left(5v_0^2-3r_1^2\right)}{r_1^7}\right)\right.\\
&\left.+\frac{7\sqrt[4]{\gamma}k\sigma u_0\left(2r_0^2-11v_0^2\right)}{r_0^{15/2}}\right],\\
F_6 =&\frac{5}{2}\gamma^{3/2}\left[7J_2^3\mu\left(\frac{J_3q_2}{r_2^9}+\frac{J_4q_3}{r_3^9}\right)+J_2\left(-\frac{3J_3\mu q_2}{r_2^7}-\frac{3J_4\mu q_3}{r_3^7}\right)-\frac{J_1(2\mu-1)q_1v_0\left(7J_1^2-3r_1^2\right)}{r_1^9}\right]\\
&+\frac{21\gamma^{7/4}k\sigma\left(-44r_0^2u_0^2+4r_0^4+55u_0^4\right)}{32r_0^{19/2}},\\
F_7 =&\frac{3}{2}\gamma^{3/2}\left[\mu\left(\frac{35J_2^2J_4^2q_3}{r_3^9}+\frac{q_2\left(-5\left(J_2^2+J_3^2\right)r_2^2+35J_2^2J_3^2+r_2^4\right)}{r_2^9}-\frac{5\left(J_2^2+J_4^2\right)q_3}{r_3^7}+\frac{q_3}{r_3^5}\right)\right.\\
&\left.+\frac{5J_1^2(2\mu-1)q_1\left(r_1^2-7v_0^2\right)}{r_1^9}-\frac{(2\mu-1)q_1\left(r_1^2-5v_0^2\right)}{r_1^7}\right]+\frac{693\gamma^{7/4}k\sigma u_0v_0\left(5u_0^2-2r_0^2\right)}{32r_0^{19/2}},\\
F_8 =&\frac{3}{32}\gamma^{3/2}\left[80\left(J_2\mu\left(\frac{q_2\left(7J_3^3-3J_3r_2^2\right)}{r_2^9}+\frac{q_3\left(7J_4^3-3J_4r_3^2\right)}{r_3^9}\right)+\frac{J_1(2\mu-1)q_1v_0\left(3r_1^2-7v_0^2\right)}{r_1^9}\right)\right.\\
&\left.+\frac{28\sqrt[4]{\gamma}k\sigma}{r_0^{11/2}}+\frac{1155\sqrt[4]{\gamma}k\sigma u_0^2v_0^2}{r_0^{19/2}}-\frac{154\sqrt[4]{\gamma}k\sigma\left(u_0^2+v_0^2\right)}{r_0^{15/2}}\right],\\
F_9 =&\frac{1}{6}\gamma^{3/2}\left[3\mu\left(\frac{q_2\left(-30J_3^2r_2^2+35J_3^4+3r_2^4\right)}{r_2^9}+\frac{q_3\left(-30J_4^2r_3^2+35J_4^4+3r_3^4\right)}{r_3^9}\right)\right.\\
&\left.-\frac{3(2\mu-1)q_1\left(-30r_1^2v_0^2+3r_1^4+35v_0^4\right)}{r_1^9}\right]+\frac{231\gamma^{7/4}k\sigma u_0v_0\left(5v_0^2-2r_0^2\right)}{32r_0^{19/2}},
\end{aligned}
$$

$$r_0 = \sqrt{u_0^2 + v_0^2}, r_1 = \sqrt{\left(u_0 - \sqrt{3}\sqrt{\gamma}\mu\right)^2 + v_0^2},$$
$$r_2 = \sqrt{\sqrt{\frac{1}{2}\sqrt{3}\sqrt{\gamma}(1-2\mu) + u_0} + \left(\frac{\sqrt{\gamma}}{2} + v_0\right)^2},$$
$$r_3 = \sqrt{\sqrt{\frac{1}{2}\sqrt{3}\sqrt{\gamma}(1-2\mu) + u_0} + \left(v_0 - \frac{\sqrt{\gamma}}{2}\right)^2},$$
$$J_1 = u_0 - \sqrt{3}\sqrt{\gamma}\mu, J_2 = \frac{1}{2}\sqrt{3}\sqrt{\gamma}(1-2\mu) + u_0,$$
$$J_3 = \frac{\sqrt{\gamma}}{2} + v_0, J_4 = v_0 - \frac{\sqrt{\gamma}}{2}.$$

Appendix II: A brief introduction of LP method

In nonlinear dynamics, the LP method serves as a widely recognized perturbation technique employed for deriving approximate solutions. This method proves particularly valuable when analyzing systems characterized by small parameters within their nonlinear differential equations, where the nonlinear terms are relatively diminutive compared to other components in the equation. Through the LP method, we can approximate the behavior of such systems by expanding the solution in a perturbation series.

Here is an in-depth elucidation of the LP method in nonlinear dynamics:

1. *Identification of the perturbation parameter* (ϵ) The initial step involves identifying a small parameter ϵ, typically representing a minute quantity within the system. This parameter is instrumental in expanding the nonlinear terms in the equation.
2. *Expansion of the solution* The system's solution is expanded as a perturbation series:

   $x(t) = x_0(t) + \epsilon x_1(t) + \epsilon^2 x_2(t) + \ldots$

   Here, $x(t)$ denotes the system's solution, $x_0(t)$ represents the zeroth-order approximation, $x_1(t)$ signifies the first-order correction, and so forth.
3. *Substitution into the original equation*: The expanded solution is substituted back into the original nonlinear differential equation, with terms organized according to powers of ϵ.
4. *Iterative approximation* By systematically solving the resulting equations at each order of ϵ, one can ascertain the corrections to the solution at each level of approximation until the desired precision is achieved.
5. *Initial conditions* The initial conditions are utilized to determine the initial values of each correction term.
6. *Computation of the solution* The final solution is derived by aggregating all correction terms.

The LP method furnishes an analytical approximation to the solution of nonlinear vibrational systems, facilitating a deeper understanding of the system's behavior. However, it is imperative to acknowledge that the applicability of this method is constrained by the small parameter ϵ, and it may not be suitable for highly nonlinear systems where the assumption of a small parameter does not hold.

Appendix III

$$G_1 = \frac{F_2\left(N_2\left(N_1+\omega^2\right)-2k\omega^2\right) - F_1\left(N_2^2+4\omega^2\right) + \omega^2\left(N_2\left(\omega^2-k^2\right) + N_1\left(N_2-2k\right) - 4k\omega^2\right)}{\omega\left(F_1\left(kN_2+2N_1+2\omega^2\right) + \omega^2\left(k\left(k^2+\omega^2+4\right)-2N_2\right) + 2N_1\left(k\omega^2-N_2\right) + kN_1^2\right)},$$
$$G_2 = \frac{-F_2\left(k^2\omega^2+2N_1\omega^2+N_1^2+\omega^4\right) + F_1\left(N_2\left(N_1+\omega^2\right)-2k\omega^2\right)}{\omega\left(F_1\left(kN_2+2N_1+2\omega^2\right) + \omega^2\left(k\left(k^2+\omega^2+4\right)-2N_2\right) + 2N_1\left(k\omega^2-N_2\right) + kN_1^2\right)} - \frac{\left(\omega^2\left(\omega^2\left(k^2+\omega^2-4\right) - 2kN_2 + 2N_1\left(\omega^2-2\right) + N_1^2\right)\right)}{\omega\left(F_1\left(kN_2+2N_1+2\omega^2\right) + \omega^2\left(k\left(k^2+\omega^2+4\right)-2N_2\right) + 2N_1\left(k\omega^2-N_2\right) + kN_1^2\right)},$$
$$H_1 = -\frac{kN_2\left(F_2+N_1+2\omega^2\right) + 2F_2\left(N_1+\omega^2\right) + 2\omega^2\left(-k^2+N_1+\omega^2-4\right) - 2N_2^2}{F_1\left(kN_2+2\left(N_1+\omega^2\right)\right) + k\omega^2\left(k^2+\omega^2+4\right) + kN_1\left(N_1+2\omega^2\right) - 2N_2\left(N_1+\omega^2\right)},$$

$$
\begin{aligned}
G_4 =& \frac{2A_{10}\left(N_2^2+16\omega^2\right)+8A_1\omega-N_2\left(G_1\left(2H_1N_3+N_4\right)+G_2\left(H_1N_4+2N_5\right)\right)}{4\omega\left(kN_2+2N_1+8\omega^2\right)} \\
&+\frac{\left(A_9+A_3A_{10}\right)\left(A_8\left(N_1+4\omega^2\right)-2k\omega\right)}{A_2\left(N_1+4\omega^2\right)}, \\
G_6 =& \frac{A_2\left(\left(N_1+4\omega^2\right)\left(G_1\left(2H_1N_3+N_4\right)+G_2\left(H_1N_4+2N_5\right)\right)\right)-2A_9\left(4\omega^2\left(k^2+4\omega^2\right)+8N_1\omega^2+N_1^2\right)}{4A_2\omega\left(kN_2+2N_1+8\omega^2\right)} \\
&+\frac{4A_1A_2k\omega-2A_{10}\left(A_3\left(4\omega^2\left(k^2+4\omega^2\right)+8N_1\omega^2+N_1^2\right)+A_2\left(N_2\left(N_1+4\omega^2\right)-8k\omega^2\right)\right)}{4A_2\omega\left(kN_2+2N_1+8\omega^2\right)}, \\
H_4 =& -\frac{A_3H_6+A_9}{A_2}, \\
H_6 =& -\frac{\left(N_1+4\omega^2\right)\left(A_2\left(2A_7+F_4G_2H_1+\left(2F_1F_3+F_4\right)G_1+2F_5G_2\right)-2A_4A_9\right)+8A_1A_2\omega}{2A_2\left(N_1\left(A_5+F_2+4\omega^2\right)+4\omega^2\left(A_5+F_2+4\omega^2-4\right)\right)+2A_3A_4\left(N_1+4\omega^2\right)},
\end{aligned}
$$

where

$$
\begin{aligned}
A_1 =& \frac{1}{2}\left(-G_2G_1N_4-G_1^2N_3-\left(G_2^2-1\right)N_5+H_1\left(H_1N_3+N_4\right)\right), \\
A_2 =& \frac{\left(F_2+4\omega^2\right)\left(4\omega^2\left(k^2+4\omega^2\right)+8N_1\omega^2+N_1^2\right)+F_1\left(8k\omega^2-N_2\left(N_1+4\omega^2\right)\right)}{2\omega\left(kN_2+2N_1+8\omega^2\right)}-4\omega, \\
A_3 =& \frac{-N_2\left(F_2\left(N_1+4\omega^2\right)+4\omega^2\left(-k^2+N_1+4\omega^2\right)\right)+8\omega^2\left(k\left(F_2+N_1+8\omega^2\right)+2F_1\right)+F_1N_2^2}{2\omega\left(kN_2+2N_1+8\omega^2\right)}, \\
A_4 =& \frac{F_1\left(kN_2+2N_1+8\omega^2\right)+4k\omega^2\left(k^2+4\omega^2+4\right)+kN_1\left(N_1+8\omega^2\right)-2N_2\left(N_1+4\omega^2\right)}{kN_2+2N_1+8\omega^2}, \\
A_5 =& -\frac{\left(kN_1+4k\omega^2-2N_2\right)\left(8k\omega^2-N_2\left(N_1+4\omega^2\right)\right)}{\left(N_1+4\omega^2\right)\left(kN_2+2N_1+8\omega^2\right)}, \\
A_6 =& \frac{\left(F_2\left(N_1+4\omega^2\right)-F_1N_2+4N_1\omega^2+16\omega^4\right)\left(2H_1^2kN_3\omega-2G_1^2kN_3\omega\right)}{4\omega\left(N_1+4\omega^2\right)\left(kN_2+2N_1+8\omega^2\right)} \\
&+\frac{\left(F_2\left(N_1+4\omega^2\right)-F_1N_2+4N_1\omega^2+16\omega^4\right)\left(H_1N_4\left(G_2\left(N_1+4\omega^2\right)+2k\omega\right)\right)}{4\omega\left(N_1+4\omega^2\right)\left(kN_2+2N_1+8\omega^2\right)} \\
&+\frac{G_1\left(F_2\left(N_1+4\omega^2\right)-F_1N_2+4N_1\omega^2+16\omega^4\right)\left(N_4\left(-2G_2k\omega+N_1+4\omega^2\right)+2H_1N_3\left(N_1+4\omega^2\right)\right)}{4\omega\left(N_1+4\omega^2\right)\left(kN_2+2N_1+8\omega^2\right)} \\
&+\frac{\left(F_2\left(N_1+4\omega^2\right)-F_1N_2+4N_1\omega^2+16\omega^4\right)\left(2N_5\left(G_2^2(-k)\omega+G_2\left(N_1+4\omega^2\right)+k\omega\right)\right)}{4\omega\left(N_1+4\omega^2\right)\left(kN_2+2N_1+8\omega^2\right)}, \\
A_7 =& \frac{\left(kN_1+4k\omega^2-2N_2\right)\left(H_1N_4\left(G_2\left(N_1+4\omega^2\right)+2k\omega\right)+2G_1H_1N_3\left(N_1+4\omega^2\right)-2G_1^2kN_3\omega+2H_1^2kN_3\omega\right)}{2\left(N_1+4\omega^2\right)\left(kN_2+2N_1+8\omega^2\right)} \\
&+\frac{\left(kN_1+4k\omega^2-2N_2\right)\left(G_1\left(N_4\left(-2G_2k\omega+N_1+4\omega^2\right)\right)+2N_5\left(G_2\left(-G_2k\omega+N_1+4\omega^2\right)+k\omega\right)\right)}{2\left(N_1+4\omega^2\right)\left(kN_2+2N_1+8\omega^2\right)}, \\
A_8 =& \frac{N_2\left(4\omega^2\left(k^2+4\omega^2\right)+8N_1\omega^2+N_1^2\right)}{2\omega\left(N_1+4\omega^2\right)\left(kN_2+2N_1+8\omega^2\right)},
\end{aligned}
$$

$$A_9 = \frac{1}{2}\left(\frac{2A_1F_1}{N_1+4\omega^2}+2A_6+F_4\left(G_1G_2-H_1\right)+F_3\left(G_1^2-H_1^2\right)+F_5\left(G_2^2-1\right)\right),$$

$$G_7 = \frac{T_1\omega\left(2F_2+kN_2+2\omega^2\right)+T_3\left(N_2\left(F_2+\omega^2\right)-2k\omega^2\right)-T_6\left(N_2^2+4\omega^2\right)}{\omega\left(F_2\left(kN_2+2N_1+2\omega^2\right)+2\omega^2\left(-k^2+\omega^2-4\right)+2kN_2\omega^2+N_1\left(kN_2+2\omega^2\right)-2N_2^2\right)},$$

$$G_9 = \frac{9F_1k\omega^2\left(3\omega\left(k^2-T_4+9\omega^2+4\right)+kT_5-2T_2\right)}{F_1\left(-F_2\left(N_1+9\omega^2\right)-9\omega^2\left(-k^2+N_1+9\omega^2\right)\right)+18\omega^2\left(2N_2-k\left(F_2+N_1+18\omega^2\right)\right)+F_1^2N_2}$$
$$+\frac{3F_1\omega\left(F_2\left(-kT_4+18k\omega^2-2N_2\right)+F_2^2k+2N_2\left(T_4-9\omega^2\right)\right)}{F_1\left(-F_2\left(N_1+9\omega^2\right)-9\omega^2\left(-k^2+N_1+9\omega^2\right)\right)+18\omega^2\left(2N_2-k\left(F_2+N_1+18\omega^2\right)\right)+F_1^2N_2}$$
$$+\frac{F_1\left(F_2\left(6\omega-T_2\right)+N_2\left(3k\omega+T_5\right)+9\omega^2\left(6\omega-T_2\right)\right)}{F_1\left(-F_2\left(N_1+9\omega^2\right)-9\omega^2\left(-k^2+N_1+9\omega^2\right)\right)+18\omega^2\left(2N_2-k\left(F_2+N_1+18\omega^2\right)\right)+F_1^2N_2},$$

$$G_{10} = \frac{T_1\omega\left(k\left(F_2+\omega^2\right)-2N_2\right)-T_3\left(N_1\left(F_2+\omega^2\right)+\omega^2\left(F_2+\omega^2-4\right)\right)+T_6\left(N_2\left(N_1+\omega^2\right)-2k\omega^2\right)}{\omega\left(kN_2\left(F_2+N_1+2\omega^2\right)+2F_2\left(N_1+\omega^2\right)+2\omega^2\left(-k^2+N_1+\omega^2-4\right)-2N_2^2\right)},$$

$$G_{12} = \frac{6\omega\left(F_2\left(N_1+9\omega^2\right)+3\omega\left(-3\omega\left(k^2+T_4-9\omega^2+4\right)-kT_5+2T_2\right)+N_1\left(9\omega^2-T_4\right)\right)}{F_1\left(-F_2\left(N_1+9\omega^2\right)-9\omega^2\left(-k^2+N_1+9\omega^2\right)\right)-18\omega^2\left(k\left(F_2+N_1+18\omega^2\right)-2N_2\right)+F_1^2N_2}$$
$$+\frac{F_1\left(-3k\omega\left(F_2+N_1-T_4+18\omega^2\right)-T_5\left(N_1+9\omega^2\right)\right)+F_1^2\left(T_2-6\omega\right)}{F_1\left(-F_2\left(N_1+9\omega^2\right)-9\omega^2\left(-k^2+N_1+9\omega^2\right)\right)-18\omega^2\left(k\left(F_2+N_1+18\omega^2\right)-2N_2\right)+F_1^2N_2},$$

$$H_9 = \frac{F_2\left(6\omega\left(3\omega\left(N_1+9\omega^2-2\right)+T_2\right)-T_4\left(N_1+9\omega^2\right)\right)}{F_1\left(-F_2\left(N_1+9\omega^2\right)-9\omega^2\left(-k^2+N_1+9\omega^2\right)\right)+18\omega^2\left(2N_2-k\left(F_2+N_1+18\omega^2\right)\right)+F_1^2N_2}$$
$$+\frac{F_1\left(N_2\left(-F_2+T_4-9\omega^2\right)+3k\omega\left(6\omega-T_2\right)\right)+F_2^2\left(N_1+9\omega^2\right)-6N_2\omega\left(3k\omega+T_5\right)}{F_1\left(-F_2\left(N_1+9\omega^2\right)-9\omega^2\left(-k^2+N_1+9\omega^2\right)\right)+18\omega^2\left(2N_2-k\left(F_2+N_1+18\omega^2\right)\right)+F_1^2N_2}$$
$$+\frac{3\omega\left(N_1\left(3\omega\left(k^2-T_4+9\omega^2\right)+kT_5\right)+9\omega^2\left(3\omega\left(k^2-T_4+9\omega^2-4\right)+kT_5+2T_2\right)\right)}{F_1\left(-F_2\left(N_1+9\omega^2\right)-9\omega^2\left(-k^2+N_1+9\omega^2\right)\right)+18\omega^2\left(2N_2-k\left(F_2+N_1+18\omega^2\right)\right)+F_1^2N_2},$$

$$H_{10} = \frac{-\left(\left(k^2+4\right)T_1\omega\right)+T_3\left(k\left(N_1+\omega^2\right)-2N_2\right)+T_6\left(kN_2+2\left(N_1+\omega^2\right)\right)}{kN_2\left(F_2+N_1+2\omega^2\right)+2F_2\left(N_1+\omega^2\right)+2\omega^2\left(-k^2+N_1+\omega^2-4\right)-2N_2^2},$$

where

$$T_1 = \frac{1}{4}\left(-G_1\left(3a_2^2N_8+3b_1^2N_6+4G_4N_3+2G_6N_4+2H_1N_7+N_8\right)\right.$$
$$\left.-G_2\left(N_7\left(3a_1^2+b_1^2\right)+2G_4N_4\right)\right)-\frac{1}{4}\left(3\left(a_1^3N_6+a_2^3N_9\right)+2\left(H_1\left(G_2N_8\right.\right.\right.$$
$$\left.\left.\left.+2H_4N_3+H_6N_4\right)+H_4N_4+2H_6N_5\right)+3G_2N_9+4G_6N_5\right),$$

$$T_2 = \frac{1}{4}G_1\left(a_2^2\left(-N_8\right)+3b_1^2N_6+2H_1\left(G_2N_8+2H_4N_3+H_6N_4\right)\right.$$
$$\left.-4G_4N_3-2G_6N_4+2H_1N_7+N_8\right)+\frac{1}{4}\left(-G_2\left(N_7\left(a_1^2-b_1^2\right)+2G_4N_4\right.\right.$$
$$\left.\left.+4G_6N_5\right)+a_1^3\left(-N_6\right)-a_2^3N_9+3G_2N_9+2H_4N_4+4H_6N_5\right),$$

$$T_3 = \frac{1}{4}\left(-3N_6\left(a_1^2H_1+b_1^3\right)+2G_4\left(2H_1N_3+N_4\right)+2G_6\left(H_1N_4+2N_5\right)-2G_2\left(H_4N_4+2H_6N_5\right)\right)$$
$$+\frac{1}{4}\left(N_7\left(-a_1^2-3b_1^2\right)-\left(a_2^2+3\right)H_1N_8-3a_2^2N_9-2G_1\left(G_2\left(H_1N_7+N_8\right)+2H_4N_3+H_6N_4\right)-3N_9\right),$$

$$
\begin{aligned}
T_4 =& \frac{1}{4}\left(-a_2^2 F_8 H_1 - 3a_2^2 F_9 + b_1^3 F_6 + b_1^2 F_7\right. \\
& - 2F_7 G_1 G_2 H_1 - 2\left(F_8 G_1 G_2 + F_4 G_4\right. \\
& \left.+2F_5 G_6\right) + F_8 H_1 + F_9) \\
& + \frac{1}{4}\left(-\left(a_1^2\left(3F_6 H_1 + F_7\right)\right) - 4F_3 G_4 H_1\right. \\
& - 2F_4 G_6 H_1 - 4F_3 G_1 H_4 - 2F_4 G_2 H_4 \\
& \left.-2H_6\left(F_4 G_1 + 2F_5 G_2\right)\right), \\
T_5 =& \frac{1}{4}\left(a_1^2\left(-F_7\right) G_2 - a_2^2 F_8 G_1 - a_1^3 F_6 - a_2^3 F_9\right. \\
& + b_1^2\left(3F_6 G_1 + F_7 G_2\right) + 3F_9 G_2 \\
& \left.-4F_3 G_1 G_4 - 2F_4 G_2 G_4\right) \\
& + \frac{1}{4}\left(2F_7 G_1 H_1 + 2F_8 G_2 H_1 - 2F_4 G_1 G_6\right. \\
& - 4F_5 G_2 G_6 + 2F_4 H_4 + 4F_3 H_1 H_4 \\
& \left.+F_8 G_1 + 2H_6\left(F_4 H_1 + 2F_5\right)\right), \\
T_6 =& \frac{1}{4}\left(-a_2^2 F_8 H_1 - 3\left(a_2^2 + 1\right) F_9 - 3b_1^3 F_6\right. \\
& - 3b_1^2 F_7 - 2F_7 G_1 G_2 H_1 - 2F_8 G_1 G_2 \\
& \left.+2F_4 G_4 + 4F_5 G_6 - 3F_8 H_1\right) \\
& + \frac{1}{4}\left(-\left(a_1^2\left(3F_6 H_1 + F_7\right)\right) + 4F_3 G_4 H_1\right. \\
& + 2F_4 G_6 H_1 - 4F_3 G_1 H_4 - 2F_4 G_2 H_4 \\
& \left.-2H_6\left(F_4 G_1 + 2F_5 G_2\right)\right).
\end{aligned}
$$

References

1. Qian, Y.-J., Guo, J.-Y., Yu, T.-J., Yang, X.-D., Wang, D.-M.: Halo orbits construction based on invariant manifold technique. Acta Astronaut. **163**, 24–37 (2019)
2. Qian, Y.-J., Liu, Z.-X., Yang, X.-D., Hwang, I., Zhang, W.: Novel subharmonic resonance periodic orbits of a solar sail in earth-moon system. J. Guid. Control. Dyn. **42**(11), 2532–2540 (2019)
3. Qian, Y.-J., Yang, X.-D., Zhang, W., Zhai, G.-Q.: Periodic motion analysis around the libration points by polynomial expansion method in planar circular restricted three-body problem. Nonlinear Dyn. **91**, 39–54 (2018)
4. Saeed, T., Zotos, E.E.: On the equilibria of the restricted three-body problem with a triaxial rigid body-I. Oblate primary. Result Phys. **23**, 103990 (2021)
5. Alrebdi, H., Dubeibe, F.L., Zotos, E.E.: On the equilibria of the restricted three-body problem with a triaxial rigid body, II: prolate primary. Results Phys. **38**, 105623 (2022)
6. Alrebdi, H., Smii, B., Zotos, E.E.: Equilibrium dynamics of the restricted three-body problem with radiating prolate bodies. Results Phys. **34**, 105240 (2022)
7. Kushvah, B.S., Kishor, R., Dolas, U.: Existence of equilibrium points and their linear stability in the generalized photogravitational Chermnykh-like problem with power-law profile. Astrophys. Space Sci. **337**, 115–127 (2012)
8. Singh, J., Richard, T.K.: A study on the positions and velocity sensitivities in the restricted three-body problem with radiating and oblate primaries. New Astron. **91**, 101704 (2022)
9. Mia, R., Prasadu, B.R., Abouelmagd, E.I.: Analysis of stability of non-collinear equilibrium points: application to Sun-Mars and Proxima centauri systems. New Astron. **204**, 199–206 (2023)
10. Vincent, A.E., Abouelmagd, E.I., Perdios, E.A., Kalantonis, V.S.: Numerical exploration of the quantized hill problem dynamics. Chaos Solitons Fractals **181**, 114688 (2024)
11. Alrebdi, H., Alsaif, N.A., Suraj, M.S., Zotos, E.E.: Investigating the properties of equilibrium points of the collinear restricted 4-body problem. Planet. Space Sci. **237**, 105767 (2023)
12. Moneer, E.M., Allawi, Y., Elaissi, S., Dubeibe, F.L., Zotos, E.E.: Equilibrium stability in the triangular restricted four-body problem with non-spherical primaries. Chaos Solitons Fractals **175**, 113933 (2023)
13. Vincent, A.E., Taura, J.J., Omale, S.O.: Existence and stability of equilibrium points in the photogravitational restricted four-body problem with stokes drag effect. Astrophys. Space Sci. **364**(10), 183 (2019)
14. Mittal, A., Aggarwal, R., Suraj, M.S., Bisht, V.S.: Stability of libration points in the restricted four-body problem with variable mass. Astrophys. Space Sci. **361**(10), 329 (2016)
15. Mittal, A., Agarwal, R., Suraj, M.S., Arora, M.: On the photo-gravitational restricted four-body problem with variable mass. Astrophys. Space Sci. **363**, 1–23 (2018)
16. Mittal, A., Pal, K., Suraj, M.S., Aggarwal, R.: Effect of stokes drag in the restricted four-body problem with variable mass. New Astron. **103**, 102042 (2023)
17. McCarthy, B., Howell, K.: Construction of heteroclinic connections between quasi-periodic orbits in the three-body problem. J. Astronaut. Sci. **70**(4), 24 (2023)
18. Abouelmagd, E.I., Alzahrani, F., Guirao, J., Hobiny, A.: Periodic orbits around the collinear libration points. J. Nonlinear Sci. Appl. (JNSA) **9**(4), 1716–1727 (2016)
19. Abouelmagd, E.I., García Guirao, J.L., Llibre, J.: Periodic orbits of quantised restricted three-body problem. Universe **9**(3), 149 (2023)
20. Salazar, F., McInnes, C., Winter, O.: Periodic orbits for space-based reflectors in the circular restricted three-body problem. Celest. Mech. Dyn. Astron. **128**, 95–113 (2017)
21. Gao, F., Wang, R.: Bifurcation analysis and periodic solutions of the HD 191408 system with triaxial and radiative perturbations. Universe **6**(2), 35 (2020)
22. Gao, F., Wang, Y.: Approximate analytical periodic solutions to the restricted three-body problem with perturbation, oblateness, radiation and varying mass. Universe **6**(8), 110 (2020)
23. Burgos-García, J., Lessard, J.-P., James, J.M.: Spatial periodic orbits in the equilateral circular restricted four-body problem: computer-assisted proofs of existence. Celest. Mech. Dyn. Astron. **131**, 1–36 (2019)
24. Suraj, M.S., Meena, O.P., Aggarwal, R., Mittal, A., Asique, M.C.: On the periodic orbits around the collinear libration points in the SCR4BP with non-spherical primaries. Nonlinear Dyn. **111**(6), 5547–5577 (2023)

25. Abouelmagd, E.I., Guirao, J.L.G., Llibre, J.: On the periodic orbits of the perturbed two-and three-body problems. Galaxies **11**(2), 58 (2023)
26. Doshi, M.J., Pathak, N.M., Abouelmagd, E.I.: Periodic orbits of the perturbed relative motion. Adv. Space Res. **72**(6), 2020–2038 (2023)
27. Sheth, D., Pathak, N.M., Thomas, V., Abouelmagd, E.I.: Periodic orbits analysis of elliptical Sun–Saturn system. Astron. Rep. **67**(5), 520–535 (2023)
28. Abouelmagd, E.I., Mostafa, A., Guirao, J.L.: A first order automated lie transform. Int. J. Bifurc. Chaos **25**(14), 1540026 (2015)
29. Ershkov, S., Leshchenko, D., Abouelmagd, E.I.: About influence of differential rotation in convection zone of gaseous or fluid giant planet (Uranus) onto the parameters of orbits of satellites. Eur. Phys. J. Plus **136**(4), 1–9 (2021)
30. Ershkov, S., Abouelmagd, E.I., Rachinskaya, A.: A novel type of er3bp introduced for hierarchical configuration with variable angular momentum of secondary planet. Arch. Appl. Mech. **91**(11), 4599–4607 (2021)
31. Ershkov, S., Mohamdien, G.F., Idrisi, M.J., Abouelmagd, E.I.: Revisiting the dynamics of two-body problem in the framework of the continued fraction potential. Mathematics **12**(4), 590 (2024)
32. Idrisi, M.J., Ullah, M.S., Kumar, V.: Elliptic restricted synchronous three-body problem (ERS3BP) with a mass dipole model. New Astron. **82**, 101449 (2021)
33. Idrisi, M.J., Ullah, M.S.: Motion around out-of-plane equilibrium points in the frame of restricted six-body problem under radiation pressure. Few-Body Syst. **63**(2), 50 (2022)
34. Idrisi, M.J., Ullah, M.S.: A study of non-collinear libration points under the combined effects of radiation pressure and stokes drag. New Astron. **82**, 101441 (2021)
35. Idrisi, M.J., Ullah, M.S.: Exploring out-of-plane equilibrium points in CRTBP: theoretical insights and empirical observations. Chaos Solitons Fractals **185**, 115180 (2024)
36. Idrisi, M.J., Ullah, M. S., Tenna, W., Khan, M. T., Khan, M. F., Kamal, M.: Out-of-plane dynamics: a study within the circular restricted eight-body framework. New Astron. 102260 (2024)
37. Idrisi, M.J., Ullah, M.S., Ershkov, S., Prosviryakov, E.Y.: Dynamics of infinitesimal body in the concentric restricted five-body problem. Chaos Solitons Fractals **179**, 114448 (2024)
38. Ranjana, K., Ullah, M.S., Idrisi, M.J.: Existence and uniqueness of solution to the system of integral equations in the planar earth, sun and satellite system. Astron. Comput. **46**, 100785 (2024)
39. Suraj, M.S., Hassan, M., Asique, M.C.: The photo-gravitational r3bp when the primaries are heterogeneous spheroid with three layers. J. Astronaut. Sci. **61**, 133–155 (2014)
40. Murray, C.D., Dermott, S.F.: Solar System Dynamics. Cambridge University Press, Cambridge (2000)
41. Beaugé, C., Ferraz-Mello, S.: Resonance trapping in the primordial solar nebula: the case of a stokes drag dissipation. Icarus **103**(2), 301–318 (1993)
42. Jeans, J.: Astronomy and Cosmogony. Cambridge University Press, Cambridge (1929)
43. Gao, F., Zhu, X., Liu, X., Wang, R., et al.: Distribution inference for physical and orbital properties of Jupiter's moons. Adv. Astron. 2018 (2018)
44. Gao, F., Liu, X.: Revisiting the distributions of Jupiter's irregular moons: I. Physical characteristics. Bulg. Astron. J. **34**, 113 (2021)
45. Gao, F., Xia, L.: Revisiting the distributions of Jupiter's irregular moons: II. Orbital characteristics. Bulg. Astron. J. **35**, 3–28 (2021)
46. Gao, F., Cheng, H.: Application of Kolmogorov–Smirnov test in the distribution of Saturn's regular satellites. Bulg. Astron. J. **37**, 76–96 (2022)
47. Gao, F., Feng, Y., Wang, R., Abouelmagd, E.I.: Analysis of motion in RTBP with variable mass based on loglogistic distribution. Result Phys. **60**, 107637 (2024)
48. Suraj, M.S., Mittal, A., Aggarwal, R.: Revealing the existence and stability of equilibrium points in the circular autonomous restricted four-body problem with variable mass. New Astron. **68**, 1–9 (2019)
49. Singh, J., Ishwar, B.: Effect of peturbations on the location of equilibrium points in the restricted problem of three bodies with variable mass. Celest. Mech. **32**(4), 297–305 (1984)
50. Suraj, M.S., Aggarwal, R., Asique, M.C., Mittal, A.: On the modified circular restricted three-body problem with variable mass. New Astron. **84**, 101510 (2021)
51. Zhang, M.-J., Zhao, C.-Y., Xiong, Y.-Q.: On the triangular libration points in photogravitational restricted three-body problem with variable mass. Astrophys. Space Sci. **337**, 107–113 (2012)